Improving the parametrization of the main channel bed roughness in the Midden-Waal

J.R. Haase

Voorwoord

Voor u ligt mijn Master Thesis. Het meesterstuk van mijn master River & Coastal engineering, geschreven in het afgelopen half jaar tijdens mijn afstudeertijd bij HKV, eigenlijk vooral in de afgelopen weken. In het afgelopen half jaar is mijn kennis over en affiniteit met de Nederlandse rivieren enorm gegroeid door de kennisintensieve onderdompeling in de morfologie van de Midden-Waal. Toen ik ruim een half jaar kennis maakte met de afstudeeropdracht in het PhD hok van Lieke had ik niet kunnen bedenken wat voor geweldige maanden er aan zaten te komen

Waar had ik nu gestaan zonder de geweldige input van alle HKV'ers die met me mee hebben gedacht. Met name Roy Daggenvoorde als dagelijks begeleider, meestal op afstand, wiens ideeën stroom niet te stoppen leek. Maar eigenlijk moet ik meer namen noemen. De goed ingevoerde lezer zal op basis van de literatuur lijst een goede gok kunnen maken.

En dat allemaal in een paar bijzondere en hectische maanden waarin ik ben getrouwd en het ouderlijk huis heb verlaten. Dank aan de vele betrokkenen om me heen die het afstuderen dan toch maar slechts een bijzaak maken!

Veel leesplezier!

Soli Deo Gloria

Joël Haase

Kampen, 16 juli 2023

Summary

Rivers are an important part of the Dutch landscape. These waterways are vital for navigation and create unique ecosystems. Water is used for domestic, industrial and agricultural purposes. Their proper management protects us from floods and the effects of droughts. As flood and drought mitigation measures are based on hydrodynamic river model simulations, accurate water level predictions from these models are needed to ensure that measures are designed in a cost-effective way. Hydrodynamic models are relatively good at predicting water levels in the discharge range for which they are calibrated. However, there is uncertainty in predicting water levels outside the discharge range for which they are calibrated. One of the main sources of this uncertainty is the uncertainty in the main channel bed roughness parameterisation.

River dunes are thought to be the main source of main channel roughness. The parameterisation of these bedforms to calculate main channel bed roughness is inaccurate as it does not account for the actual bedforms. The bed is parametrised using implicit 2D river dune geometry parameters by estimating these parameters as a function of water depth. A 2D parameterisation often only captures the dunes on the centreline of the fairway, while the centreline of the fairway is not representative of the entire river bed, resulting in an inaccurate roughness prediction (1).Furthermore, the implicit bedform covers the discharge history dependent bed evolution in the hydrodynamic river model D-HYDRO, which has a large influence on the main channel bed roughness, as extreme discharge events are not accurately simulated, while these events are of great interest (2). Finally, the length scale over which roughness is assumed to be constant is too large to capture the spatial variation in bedforms (3).

Each of these three problems was assessed in the study area of this research, the Midden-Waal.

1. Using a dataset of bed measurements taken approximately every two weeks in the years 2018-2020, 2D river dune statistics were compared with 3D river dune statistics to analyse the potential added value of bed parameterisation.
2. The roughness estimation formula in D-HYDRO was extended with a term capturing the influence of discharge history by multiplying the roughness estimate with a dimensionless discharge (history) dependent factor: Q/Qhis. The length of the discharge history was based on the bedform turnover time, which has a wide bandwidth. A sensitivity analysis was carried out to determine the most appropriate period.
3. New roughness sections were defined in the Midden-Waal based on the trend in dune height to increase the physical nature of the calibrated roughness. These sections were calibrated and the calibrated roughness was compared with bedform statistics to extract potential relationships.

Parametrising the river bed with 3D statistics did not result in usable bedform statistics. The 2D dune height appeared to follow the same trend as the 3D dune height, but the 3D dunes were higher compared to the 2D dunes, probably due to the way the statistics were derived. Different locations in the study area result in comparable dune heights.
2D dune length was compared with 3D dune area and 3D dune length. The 3D dune height at the beginning of the Midden-Waal increased with increasing 2D length, but somewhere in the middle of the study area the relationship between 2D length and 3D area appeared to be almost a horizontal line, indicating that either the bed development is site specific or the methodology should be revised. The comparison between 2D and 3D length showed that the 3D dunes had much shorter lengths, because this length was determined by averaging the length of the whole 3D dune in the flow direction.

Overall, the parameterisation of the river bed in 3D did not lead to any new insights, but the concept should not be discarded yet, as more research is needed to fully exploit the potential of 3D dunes.

The roughness estimate in D-HYDRO can be improved by adding the discharge history to the current roughness estimate. Using the averaged discharge over 50 days (median bedform turnover time) gave the best roughness estimate. For longer periods >75 and shorter periods <25 days the added value of the discharge history became marginal. In agreement with the literature, dune steepness was found to add value to the roughness estimate.

The calibration of the new roughness sections in the Midden-Waal did not lead to new insights in the roughness-bedform relationship, as the calibrated roughness had an unexplainable large peak around 1350 m3/s, which made it impossible to relate the calibrated roughness to bedform statistics. Therefore, the original roughness section was used for the final step of this research.

The combination of all the knowledge gained led to a final formula for the three roughness sections in the unchanged D-HYDRO model with discharge fraction and dune steepness as variables. The free coefficient varied in the same trend as the dune height, increasing the physical nature of the formula. The results show that there is room for improved, physically based roughness estimates in the Midden-Waal. Further research on new roughness sections and an improved parameterisation of the riverbed could improve the results even further.

Table of contents

1. Introduction

1.1 Relevance of research

Rivers are an important part of the Dutch landscape. These waterways are vital for shipping and create unique ecosystems. Water is extracted for domestic use, industry and agriculture. Sophisticated river management is necessary to protect us from flooding and to maintain the various functions of our waterways in a cost-effective way. Climate change complicates this management. High flows will become more extreme and periods of low flows will last longer (Parmet et al., 1995; Huang et al., 2015). Higher peak flows make flood risk reduction more challenging, while low flows may impede navigation and degrade water quality.
A major tool in the design of flood protection and water level predictions are hydrodynamic models. These models are able to reproduce water levels for the discharge range for which they are calibrated. However, predictions of water levels for discharges outside the calibrated discharge domain are uncertain. Yet, accurate predictions of water levels are needed to ensure that mitigation measures are properly designed, such that they are not over- or undersized, with the associated social and economic consequences. Therefore, the uncertainty water level predictions for discharges outside the calibrated reach should be reduced, by increasing the reliability of the outcomes of hydrodynamic river models. Improving our hydrodynamic river models is crucial in order to adapt to the even more complex challenges posed by climate change and to ensure the proper management of our waterways.

1.2 Towards the research gap

1.2.1 Hydrodynamic models

Hydrodynamic models are used to calculate the water depth in a river given a certain input hydrograph. The uncertainty in the calculated water depth can be attributed to model errors and the uncertainty in the input parameters. In recent decades, model errors and uncertainty in the outcomes have been reduced by decreasing the time step and increasing the resolution of grid cells and quality of input data, and by adding more physical processes (Hardy et al., 1999; Bridge, 2003; Neal et al., 2012; Bomers et al., 2019). However, hydrodynamic river models are still not able to reproduce measured water levels well when relying on these inputs only (Warmink, 2011; Domhof et al., 2018).
One of the most uncertain input parameters is the hydraulic roughness of the main channel and the floodplain (Horritt & Bates, 2002; Warmink et al., 2013). Within the main channel, bed material, bedforms and human structures such as groynes are dominant sources of roughness, whereas in the floodplain, vegetation, human structures and other elevated objects induce friction (Berends et al., 2018; de Lange et al., 2021). Because roughness is the most uncertain parameters, it is often used for calibration (Warmink, 2011; Domhof et al., 2018).

1.2.2 River dunes

The main source of hydraulic roughness in the main channel is form drag due to river dunes (Paarlberg et al., 2010; de Lange et al., 2021). River dunes are triangular periodic bed features that are in continuous interaction with the flow (Naqshband et al., 2017; Lokin et al., 2022).
The flow-induced sediment transport propagates and evolves the dunes over time. Depending on the bed-flow interaction, river dunes will grow, decay or propagate (McElroy & Mohrig, 2009; Naqshband et al., 2017). The changing geometry and flow characteristics in time and space complicate the understanding and prediction of dune evolution and interaction in rivers.

Over the last decade, the understanding of dune interaction and behaviour under varying flow conditions has improved. Dunes can form spontaneously, split, pass through each other, merge or die out (Warmink, 2014; Reesink et al., 2018) . Contrary to the belief that the aspect ratio between dune height and dune length is constant (Van Rijn, 1984; Bradley & Venditti, 2017), Warmink (2014) observed hysteresis in dune height and dune length while adapting to flow conditions: The height of a dune adapts faster than its length, resulting in higher roughness values at the peak of a flood wave. Faster changes in discharge in a flood wave in result in larger hysteresis than gradual changes. Lokin et al. (2022) showed that dunes become longer during low flows, implying that the bedform induced roughness decreases as the low flow continues. It can be concluded that discharge history is an important factor in the evolution of river dunes.

1.2.3 River dunes and roughness relationships

Several empirical relationships exist that relate dune geometry, dune height (H) and often dune length (L) as well, to a roughness coefficient (Vanoni & Hwang, 1967; Engelund, 1977; Van Rijn, 1984; Soulsby, 1997; Bartholdy et al., 2010). Lefebvre & Winter (2016) found that the lee side angle determines the magnitude of flow separation, and proposed a correction factor as a function of the lee side angle. However, none of these relationships are able to fully explain the variation in hydraulic roughness, indicating that dune morphology is not the only relevant factor in explaining the variation in hydraulic roughness (de Lange et al., 2021). However, additional sources of roughness are not understood sufficiently well too to explain measured water levels, so the hydraulic roughness remains uncertain (Domhof et al., 2018). Besides, since the contribution of sources of roughness is discharge dependent (Niesten et al., 2022), the identification of contributions of other sources gets even harder.

1.2.4 Roughness in hydrodynamic river models

Due to this complexity and limiting knowledge on contribution of sources of roughness, the hydraulic roughness parameter in hydrodynamic river models is still a calibrated value, valid only for the conditions which are used for calibration. Thus, water levels within the calibrated reach can be estimated relatively well, but the prediction of extreme high and low water levels outside the calibrated reach remains uncertain. Uncertainty additions are required to deal with this uncertainty in the extreme range, e.g. to determine the design water level used to design flood defences or other hydraulic structures. When the model uncertainty is reduced, these uncertainty additions could be reduced as well, leading to a lower required crest height, which will involve large cost reduction.

In the latest (6^{th}) generation of hydrodynamic river models in the Netherlands, the roughness parameter is not a fully calibrated value, but a roughness estimate based on bed characteristics, calibrated with a multiplication factor which is determined for 5 discharge levels: [800, 1580,2400, 5350, 7200] m^3/s (Niesten et al., 2022).
The roughness estimate is not real time bed characteristics based, since it is not possible to include actual, bedforms during a simulation, it is assumed that bedform characteristics can be estimated being as function of the water depth. The roughness estimate is calibrated with a calibration factor. The calibration factor is interpolated between the calibrated discharge levels, because it is determined for 5 discharge levels only.

Figure 1 shows the roughness estimate and the calibrated roughness for the section of the Midden-Waal between Nijmegen and Dodewaard, both as function of the discharge. A Qh relation based on the discharge and water level data obtained from the measuring station of Tiel was used to link discharge and water depth in this formula. The values for the calibration multipliers for the 5

discharge levels are [0.854, 0.907, 0.94, 0.942, 0.897] respectively (Niesten et al., 2022). The roughness estimate used in D-HYDRO is a function of water depth (h) only:

$$k_s = Ah^{0.7}\left(1 - e^{-Bh^{-0.3}}\right) \quad \text{EQ. 1}$$

k_s is the Strickler roughness height. The values used for formula coefficients A, B are 0.083 and 2.5 respectively, for this river section (Niesten et al., 2022). This equation is built such by the model developers that it approaches the outcomes of the bed roughness equation of Van Rijn (1984):

$$k_s = 3D_{90} + 1.1H\left(1 - e^{-\frac{25H}{L}}\right) \quad \text{EQ. 2}$$

With the 90th percentile of the grain size (D_{90}), the dune height (H) and the dune length (L) as input values. The model developers used value for these three input variables based on bed measurements in the Waal. By using the equation of Van Rijn as a target, the model developers created as physics based estimate which is easily implementable in D-HYDRO since the only variable is the water depth.

It can be seen that the calibrated roughness is quite different from the roughness estimate, indicating that the roughness estimate may be improved. The unknown uncertainty outside the calibrated reach is denoted with the green area.

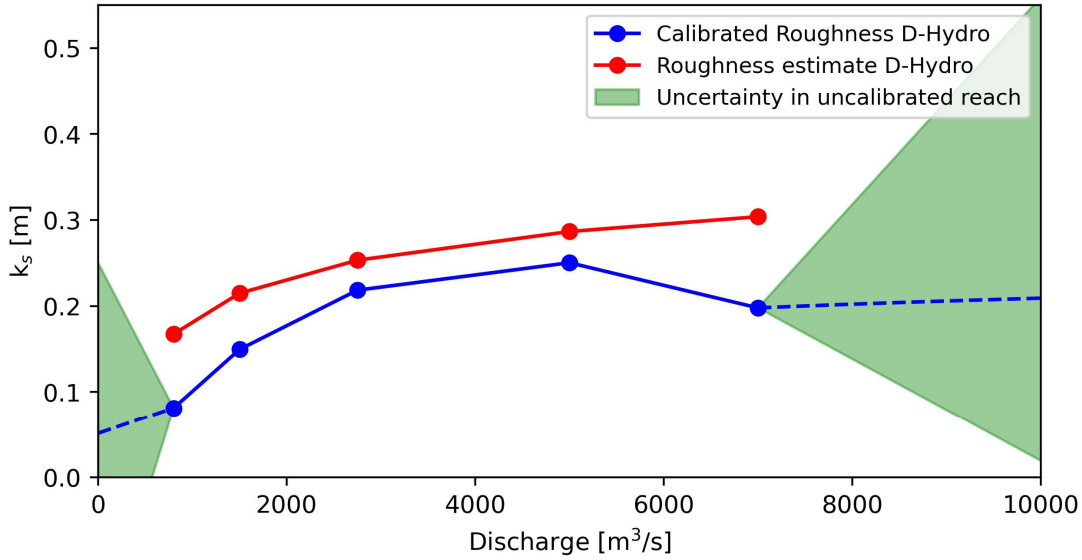

Figure 1 Roughness estimate and calibrated roughness in D-HYDRO between Nijmegen and Dodewaard. Based on equation 1. The calibration factors are different for each of the 5 discharge levels [800, 1580, 2400, 5350, 7200] m^3/s . During a simulation, D-HYDRO interpolates between the 5 calibrated roughness height. The green area indicates that there is uncertainty in the uncalibrated discharge reach.

1.2.5 Calibration of main channel roughness

The aim of the model developers was to base the roughness estimate (EQ. 1) on the local characteristics of the river. Bedform characteristics and grain size distribution were implicitly included a simplification of the van Rijn formula, as described above. However, calibration was still necessary, as was presented in Figure 1.

Figure 3 shows the calibration factors for the 5 discharge levels, varying for each calibration trajectory in the Waal. The spatial distribution of the calibration trajectories in the Waal can be found in Figure 2. These trajectories correspond to the sections between the LMW (Landelijk Meetnet Water) gauging stations.

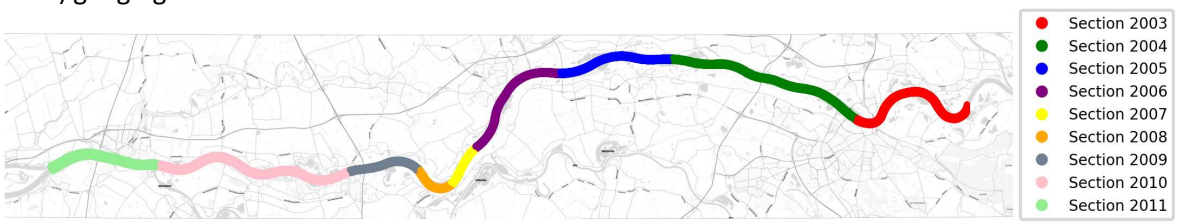

Figure 2 Calibration trajectories in the Waal. Sections are between the LMW gauging stations.

In the current model, trajectories 2006-2009 are calibrated all at once. This can also be seen in Figure 3, these 4 section have the same calibration factor. However, these section may be split up later due to river interventions (Niesten et al., 2022).

The calibration factor currently lacks consistency, showing spatial overlap and inconsistent variations with discharge across trajectories. This inconsistency highlights a limitation in the roughness estimation provided by Equation 1, as it overlooks localised roughness variations and discharge-dependent contributions.

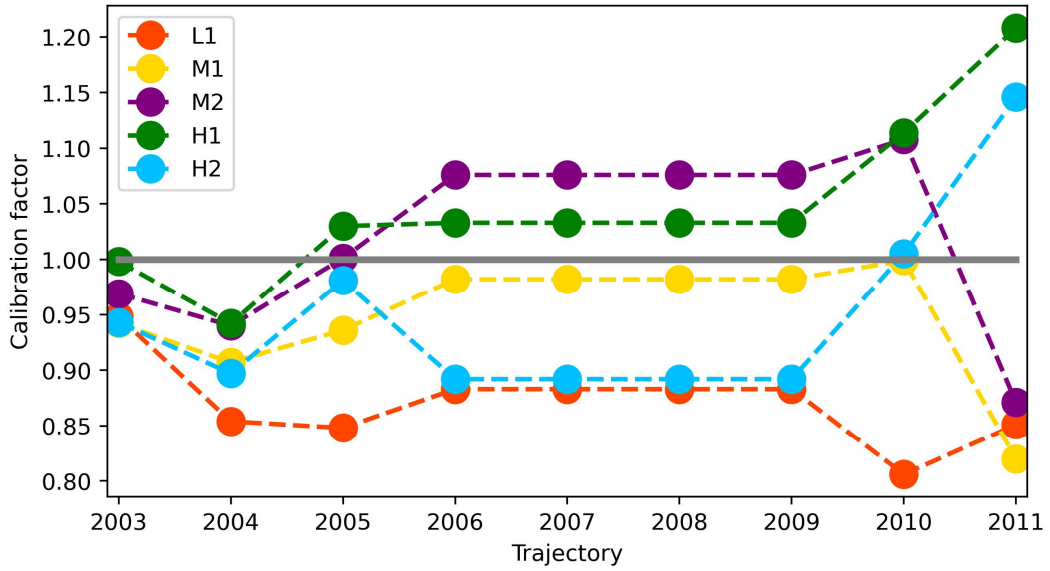

Figure 3 Calibration factors for the Waal for each of the 5 discharge levels (low (L_1), medium ($M_{1,2}$) and high ($H_{1,2}$)), varying per trajectory along the river. Trajectory boundaries per trajectory correspond to the locations of the LMW stations. Adapted from Niesten et al. (2022)

1.3 Research gap

The simplified formula of Van Rijn assumes that dune dimensions and grain size are a function of water depth only, which is not in line with the previously described results of Warmink (2014) and Lokin et al. (2022). This decreases the physical nature of the roughness description, as the geometry of river dunes depends on the discharge history and dune length is not a linear function of the water depth(Lokin et al., 2022). Roughness estimates should therefore be directly based on geometry, or a discharge history dependent variable should be added to a roughness estimate like Equation 2 to implicitly include actual dune geometry.

Moreover, until now, bed form roughness is parametrized with use of 2D river dune parameters (dune height and length in flow direction, see Equation 2). Especially when only the centre axis of the fairway is used to determine these characteristics, the estimated roughness may not be representative because the river bed changes over width. Using statistics that parametrize bedforms in 3D might increase the physical nature of the main channel roughness in hydrodynamic river models as the river bed is parametrized in more detail.

Another limitation is the length scale at which roughness values are assumed to be constant. The coefficient A in EQ. 2 is derived by scaling the average dune height over trajectories greater than 10 km (see red line in Figure 4). Verberk et al. (2023) showed that dune development is location dependent and suggested roughness sections smaller than 4 km to ensure that local bed geometry is better accounted for. The grey scaled scatter of the unaveraged scaled dune height in Figure 4 supports this.

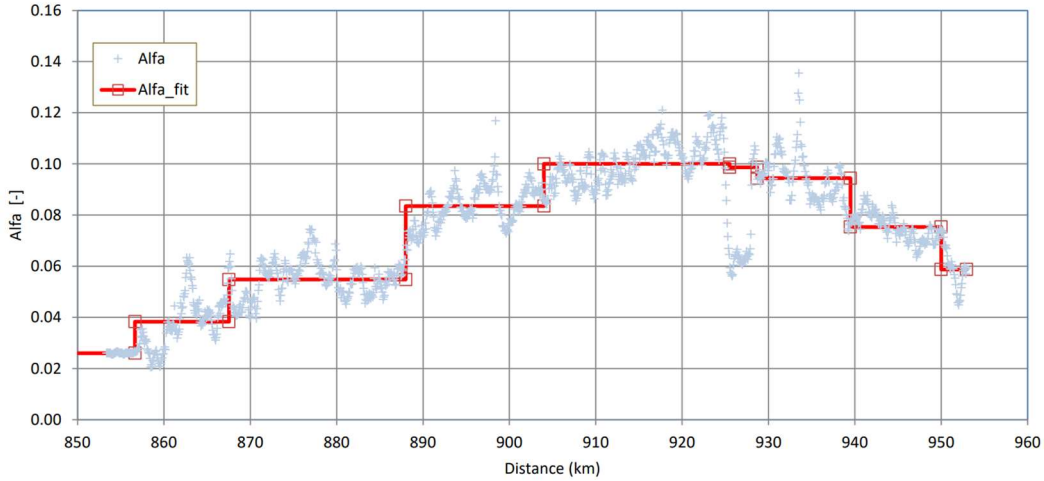

Figure 4 Spatially varying formula coefficient A (red line), determined by using the averaged scaled dune height along the river. Averaged dune height values are scaled to a maximum value for A of 0.1 based on calibration experience (Niesten et al., 2022).

Figure 5 Roughness estimate trajectories.

Summarizing, the current way in which is dealt with main channel bed roughness does not capture the influence of discharge history in the description of bedforms. Moreover, using a 3D parametrization of the bed might improve the physical nature of the bed roughness. Lastly, when bed roughness is assessed on smaller scale, the inclusion of local river characteristics might improve the roughness parametrization.

1.4 Problem definition

Accurate prediction of water levels in rivers is essential for effective river management. However, there are uncertainties in the predictions, especially in the uncalibrated discharge domain. One of the main problems at hand is the inadequate representation and understanding of hydraulic roughness in hydrodynamic river models. The limitations in accounting for the complex dynamics of river dunes, the inability to fully explain the variation in roughness, and the lack of spatial consistency in roughness calibration hinder accurate water level predictions beyond the calibrated reach. Addressing these challenges is crucial to enhance the effectiveness and reliability of river management strategies, including flood risk reduction and the design of hydraulic structures.

1.5 Hypothesis

Once calibrated, hydrodynamic models are able to reproduce measured water levels relatively well. However, it is not known which processes are captured behind these calibration factors. Therefore, any insight in these processes will help to reduce the model uncertainty. Based on the research gap, 3 hypotheses are defined:

1. 3D river dune parametrization improves the current 2D approach
2. Adding discharge history to the roughness formula will decrease the calibration factor and decrease therefore the model uncertainty.
3. Smaller roughness sections based on characteristics will increase the physics-based nature of the main channel roughness.

1.6 Research objective and research questions

To provide a physical basis for improved modelling and river management strategies in the extreme discharge domain, the research objective is to investigate the relationship between discharge and river bed induced roughness in the measured discharge domain (1000-11800 m3/s at Lobith) so that the uncertainty in the predictions of water levels in the extreme discharge domain is reduced. The main assumption in this research is that the main channel roughness is only caused by bedforms. The research objective and research gap combined with this main assumption, leads to the following research question:

"To what extent can the degree of calibration for hydrodynamic river models be reduced by using improved parameterisation of bedforms, discharge history and physics-based roughness sections in the estimation of bed roughness for the river Waal?"

The following sub-questions arise from this main research question:

1. To what extent does the use of 3D bed parameterisation statistics, as opposed to 2D dune statistics, provide additional information that reduces the degree of calibration?
2. To what extent does the inclusion of discharge history in the main channel bed roughness parameterisation reduce the degree of calibration required?

3. To what extent does the use of physically based roughness sections help to reduce the degree of calibration required?
4. To what extent can the combined findings from the previous research questions be used to reduce the degree of calibration required for main channel roughness parameterisation?

A flow chart of these 4 research questions is shown in Figure 6. Research questions 1, 2 and 3 are three independent parts of the research based on the research gap, while the last research question combines all the knowledge gained in the establishment of a final roughness formula, which should be an improvement over the current way of estimating roughness prior to calibration.

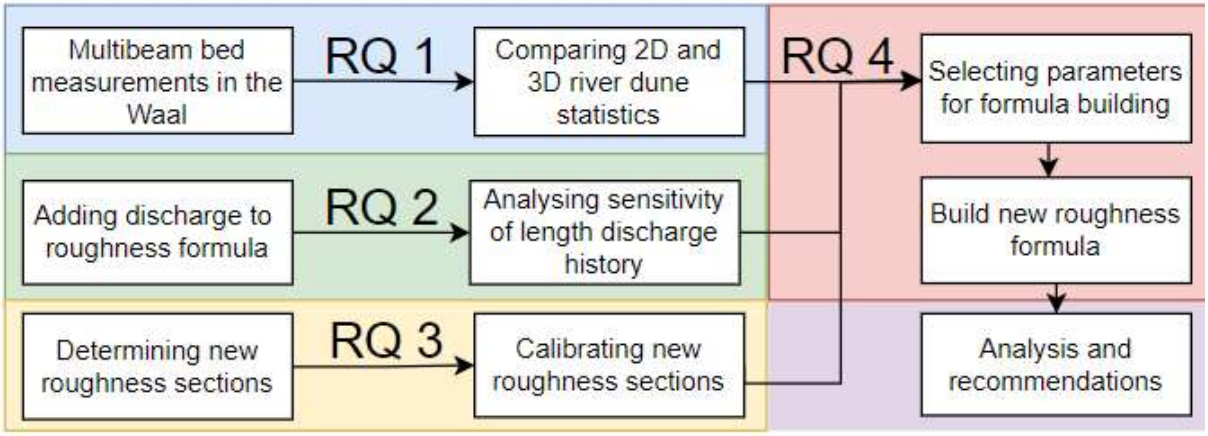

Figure 6 Flow diagram of the 4 research questions

1.7 Report outline

The outline of this report is as follows. The first chapter was the introduction, where, based on literature research, a research gap, a problem definition and hypothesis were defined. This formed the basis of the research objective and the research questions. In the second chapter, the used methodology is described for each of the research questions. In the third chapter, the results are described per research question. In chapter 4 and 6, the discussion, recommendations and conclusions.

2. Method

2.1 Study area

The Midden-Waal was the study area of this study (see Figure 7). This area was chosen because processed Multibeam Echo Sounding data were available. This section of the Waal is located roughly between river kilometre 894 and 911, almost 17 km long and relatively straight with some slight bends. The two bridges over the Waal enclose the study area. A third option for crossing the river is a small ferry, which is accessible to hikers and bikers. What stands out are the 'harbours' that are connected to the river or integrated as 'lakes' in the floodplain. There are fewer of these around Nijmegen and Tiel. In this part of the river there are no longitudinal training dams, as is the case downstream of Tiel. However, there are groynes every 200 metres.
In and around this study area there are three Rijkwaterstaat gauging stations, indicated by the blue dots. At these stations the water level is measured every 10 minutes.

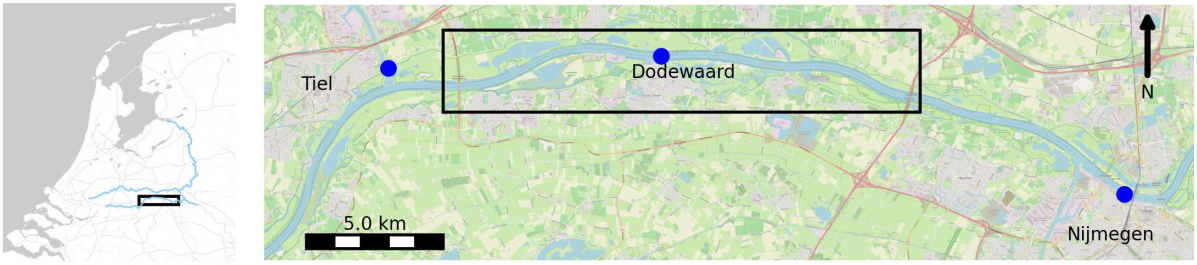

Figure 7 Area of interest in this study. Midden-Waal, some kilometres downstream from Nijmegen, is located between the bridges of the roads A50 & N323. The blue dots indicate where the measurements are conducted by Rijkswaterstaat

2.2 Model

In the introduction, the hydrodynamic model that was analysed and going to be used was already mentioned: D-HYDRO, which is the same model as Delft 3D FM. The model development was described in Niesten et al. (2022). An important element in this research was the calibration performed by the model developers. From now on, the model, as received from Deltares, will be called the **'default model'**. In this report, often will be referred to the roughness estimate in the default model, or the calibrated roughness in the default model.

2.3 Data

To analyse the bed characteristics of the Midden-Waal, a dataset of processed multibeam bed measurements was used. This dataset contains 58 measurements, which were taken approximately every two weeks in the period between 2017-11-01 and 2020-02-01. The multibeam bed measurements had already been processed into stream coordinates (relative to the beginning of the Midden-Waal) for the study by Lokin et al. (2022). The data were projected onto a 1 x 1 m grid and processed according to the standards (de Ruijsscher et al., 2020). Only the middle 150 metres of the fairway are used in this study, in order to avoid possible effects of groins on the bed development and therefore on the results. For the sake of clarity, the entire Midden-Waal was projected on a 1 x 1 grid, so that a dataset with bed elevations of 16750 m (length of the Midden-Waal) x 150 m (middle 150 m of the fairway) cells was used in this study.

Discharge and water level data were obtained from the gauging stations mentioned in the previous section. Stage relation curves (version 2018) were used to interpolate water levels between the gauging stations (Rijkwaterstaat, 2023).

Figure 8 shows the moments for which bed measurements are available. The green dotted line indicates the discharge at which the floodplains start to be inundated: ~2500 m^3/s. 95% of the measurements were taken at discharges below 2500 m^3/s. Therefore, the study was limited to bed measurements at discharges below 2500 m^3/s in the Waal, as relationships between the bed and higher discharges would not be as strongly supported by the data as in the case of lower discharges.

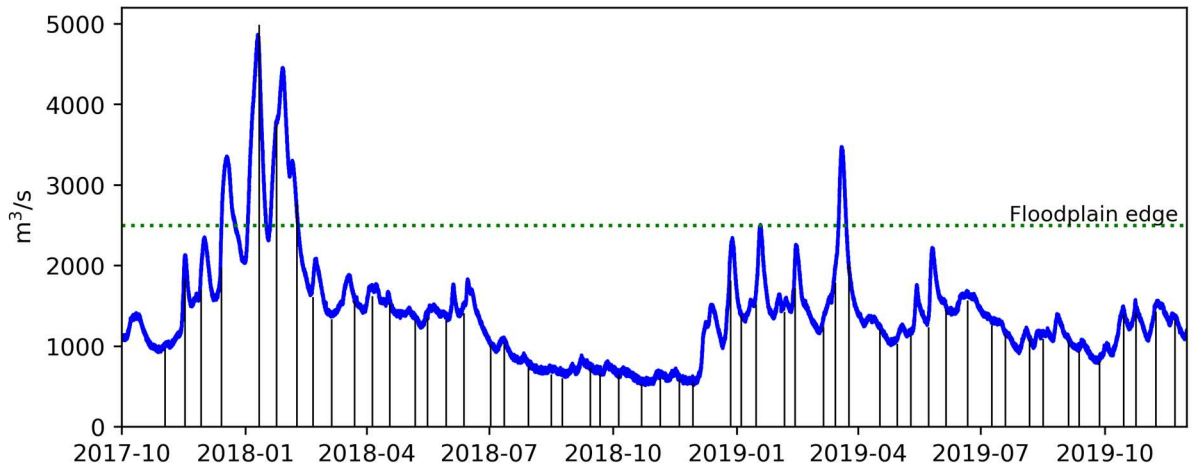

Figure 8 Discharge in the Waal and moments on which Multibeam Bed measurement were conducted. Green dotted line indicates the discharge at which the floodplain starts to inundates: 2500 m^3/s.

As the calibration of the latest version of D-HYDRO the Waal is only performed for the main channel roughness parameter, errors in the floodplain roughness parameterisation are compensated during the calibration of the main channel roughness coefficient for discharges higher than 2500 m^3/s (Niesten et al., 2022). Therefore, restricting our discharge range of interest to 2500 m^3/s reduces the uncertainty in the assumption that the main channel roughness in the Waal is only caused by bedforms because errors in the flood plain roughness parametrisation do not affect the results.

2.4 RQ 1: 2D dunes vs 3D dunes

This section describes the methodology used to answer the first research question. The aim of this first research question was to compare 2D and 3D dune statistics to determine whether 3D statistics are an improvement over 2D statistics.

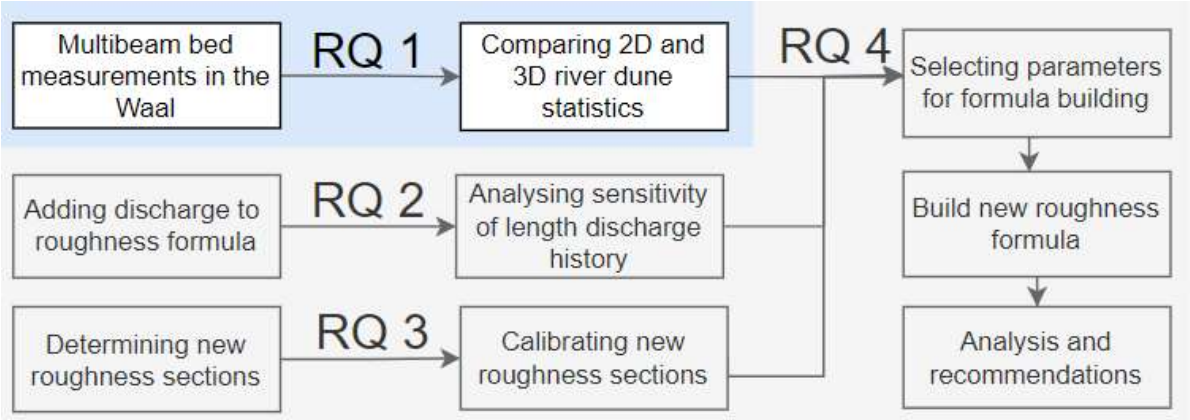

2.4.1 2D dune statistics

The main channel roughness is mainly caused by river dunes (Paarlberg et al., 2010; de Lange et al., 2021). Until now, river dunes have always been assessed as 2D features with a height, length and lee slope angle. These geometric features can be used to calculate bedform induced roughness using one of the available bedform roughness predictors, mentioned in the introduction. In this study, 2D dune statistics were used as in Lokin et al. (2022). Dune height was defined as the height of a dune crest relative to the next trough. Dune length was defined as the distance between the two adjacent troughs of a dune crest.

2D dune statistics were determined for the centre axis of the fairway and averaged per 2 km section, as was suggested by Haase et al. (2023): Larger sections do not capture the spatial variation in dune statistics well, while too much detail is not necessary and does add much value.

2.4.2 3D dune statistics

In addition to 2D shape parameters, dunes can also be treated as 3D features with parameters such as height and size. This provides an opportunity to improve the parametrisation of the main channel bed geometry, as the central axis of the river or the centre of the fairway is often used to determine 2D shape parameters representing the whole river bed (de Lange et al., 2021; Lokin et al., 2022). See Figure 9 for an impression of the river bed.

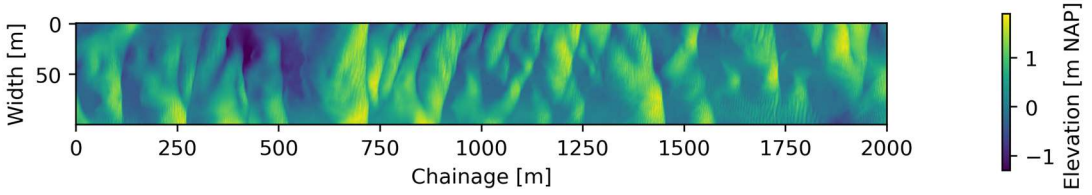

Figure 9 Section of 2 km in the middle of the Midden-Waal. Chainage is the streamwise length of this section. Width is the middle 100 m of the Waal with the middle axis of the fairway as the centre line.

The 3D parameters to be extracted were: height, size and length in flow direction. Other 3D parameters could have been determined. However, this was beyond the scope of this study. After dividing the river into 2 km sections, the 3D dune shape parameters were determined as follows:

1. For analysis purposes, the bed elevation was modified by using the slope of the Waal, which is approximately $1.1 \times 10^{-4}\ m/m$ (Domhof et al., 2018) ($slope \times distance_{ref}$) so that the

bed is no longer sloping but straight, with the upstream edge of the Midden-Waal as the reference elevation in meters + NAP.

2. To determine the 3D dune height, the local maxima were determined. A local maximum was defined as a grid cell where all neighbouring grid cells have a lower elevation. It was important to decide which local maxima to use to determine the 3D dune height, as there could be one local maximum in an erosion pit, or 2 local maxima only 2 metres apart. The first point of interest will be assessed now, while the second will be assessed in the next, the third point.
   The 90th percentile of bed elevation was used as a threshold to determine which cells were identified as local maxima. This percentile ensures a balance between retaining enough maxima during low flows (elevation becomes more uniform as dunes become longer and lower (Lokin et al., 2022)) and too many maxima as relatively unimportant elevated parts of the river are identified as 3D dunes, which are mainly responsible for inducing shape drag. The threshold percentile was not based on literature (no literature available) or chosen at random, but was the result of an iterative process of visual inspection where the percentile was changed until a balance was achieved between the number of peaks during high and low flows.
   The height of the peaks was determined by subtracting the height of the peaks from the 15th percentile of height per section analysed. This percentile ensures a balance between defining the height of the peaks relative to the bed as neither too high nor too low.
3. The area of a dune was determined by using a search algorithm that searched around a local maximum until the edge of cells below the 85th percentile of the elevation was found. The number of cells within the elevation contour represents the surface area of a dune in m^2. As with the determination of the dune height threshold,, the contour percentile should not be set too low or too high, resulting in small dunes at high discharges or very large dune areas at low discharges. also determined with an iterative process of visual inspection of the outcomes. If this percentile was set too high, the dune area was very small, while a lower percentile resulted in unnecessary dune merging.
   If the area around a local maximum contained several other local maxima, only the highest dune peak was selected to avoid identifying the same dune more than once. An impression of the location of the identified dune peaks and the elevation contour around these peaks is given in Figure 10
4. For each dune, the mean length in the stream direction was determined by averaging the distance from the upstream and downstream edges of each dune contour.

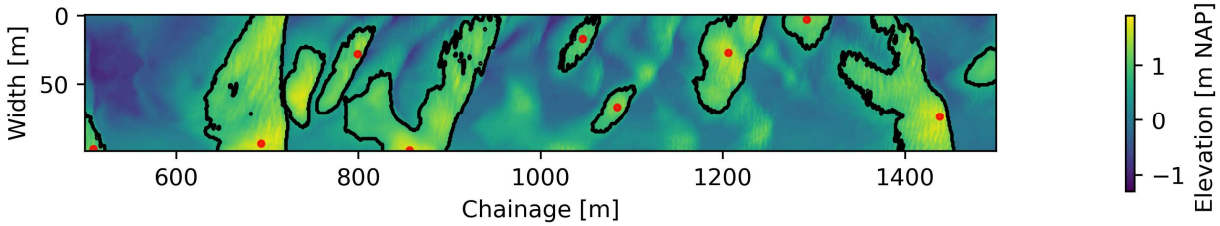

Figure 10 Snapshot of the river bed shown in Figure 9. The red dots show the local maxima above the 95th percentile of bed elevation in the whole snapshot, at least 40 metres apart. The black contour indicates the 85th percentile of elevation, which determines the surface area of a dune.

2D and 3D dune height were compared, while 2D length was compared with 3D size and 3D length. An analysis of the difference per parameter was performed to determine if the 3D approach added new information compared to the 2D approach. The potential relationship with the calibrated roughness in the standard model was also investigated.

2.5 RQ 2: The inclusion of discharge history

In this section the methodology used to analyse the potential added value of discharge history to the main channel bed roughness estimate is presented. The aim of this research question was to determine whether the addition of discharge history to the current roughness formulation would reduce the level of calibration required.

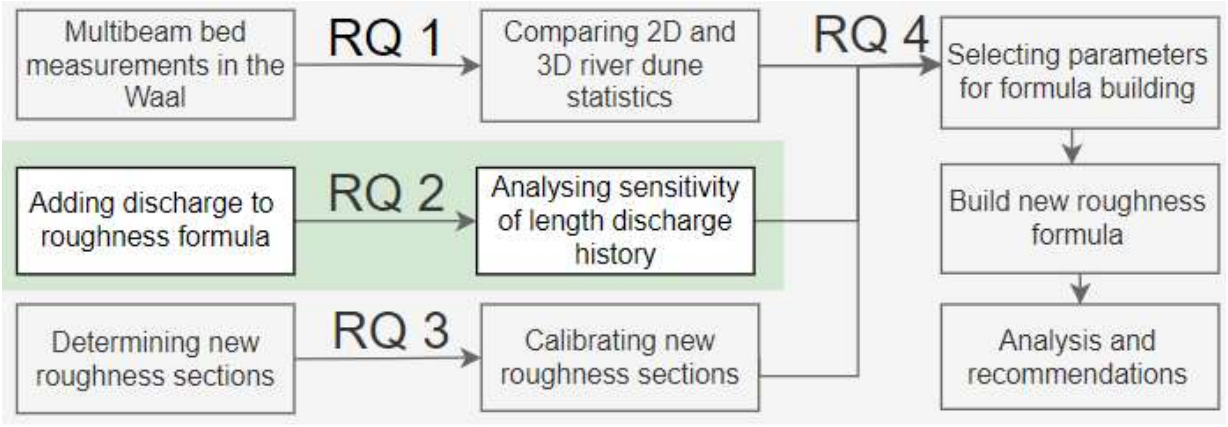

2.5.1 New formula

The current way of estimating roughness in D-HYDRO is via Equation 1 (Niesten et al., 2022). As mentioned above, this equation assumes that dune geometry can be estimated proportionally to water depth, which is not the case as discharge history has a large influence on river bed evolution. Therefore, an extension of the current roughness estimation has been proposed to capture the influence of discharge history:

$$\boldsymbol{k_{s\,new} = A_{new} h^{0.7} \left(1 - e^{-B_{new}\ h^{-0.3}}\right) \times \left(\frac{Q}{Q_{his}}\right)^{P1}} \qquad \text{EQ. 3}$$

The new term in this equation consists of some new/updated elements, which will be described shortly:

- A_{new} and B_{new}, an update of the existing formula coefficients A and B. For analysis purposes, each coefficient was allowed to vary freely, to obtain the best fit. The way in which the new coefficients were determined will be described later on.
- Q. In order to be able to include bedforms later on in the processes, the roughness height k_s was only calculated for the moments where bed measurements were available (see Figure 8). Each bed measurement could be associated with a discharge Q, which is included in the extended roughness estimate
- Q_{his}. Bedforms are a result of the interaction of the flow with the bed. Q_{his} is the mean discharge over a period of time prior to each bed measurements. The output of the discharge fraction $\frac{Q}{Qhis}$ therefore determines the value of the discharge at the time of each bed measurement, relative to the mean discharge over a period of time. The length of the discharge period will be discussed later on.
- $P1$. This formula coefficient determines the influence of the discharge fraction on the roughness estimate. The closer the value of P1 to zero, the smaller the influence of the discharge fraction. The way in which the value of this coefficient has been determined will be explained later.

Adding a term such as the dimensionless discharge history fraction Q/Q_{his} maintains the structure of the formula as no stand alone terms are added. This prevents us from overfitting the roughness estimate.

The aim of this extended formula was to produce a roughness estimate by reverse engineering: using the calibrated roughness as a target for parameterising a new roughness estimate. This meant that the coefficients in the formula were optimised to be as close as possible to the calibrated roughness. Appendix C elaborates on this reverse engineering method.

2.5.2 Roughness target

The target roughness is a multiplication of the spatially varying background roughness and the spatially varying calibration factor (Niesten et al., 2022). The following equation was used to calculate the target roughness:

$$\boldsymbol{k_{s\,target} = Ah^{0.7}\left(1 - e^{-Bh^{-0.3}}\right) \times \left(C_{fac}\right)^{6}} \qquad \text{EQ. 4}$$

The first part of this equation is already known as the roughness estimate in the default model. The calibration factor (C_{fac}) and the 6th power requires some additional explanation. All roughness definitions in D-HYDRO are converted to a Manning coefficient before being used in the impulse equations (Niesten et al., 2022). This was also done for the roughness estimate, prior to the calibration procedure. As the conversion between a Strickler roughness (k_s) and a Manning coefficient (n) is often done via Equation 5. A 6th power was used to convert a calibrated Manning coefficient back to the calibrated Strickler roughness height. An example of the spatial and discharge dependent calibration factors can be found in Appendix A, Figure 29.

$$\boldsymbol{n = 0.04\, k_s^{\frac{1}{6}}} \qquad \text{EQ. 5}$$

The first step was to couple the spatial characteristics of the roughness estimate (Eq. 1) with the spatial characteristics of the calibration factors. Figure 11 shows the spatial distribution of the background roughness. Figure 12 shows the spatial distribution of the calibration factors. As mentioned earlier, the roughness estimate trajectories are determined based on a trend in dune height in the Waal while the trajectories for the calibration factors are defined between the gauging stations of Rijkswaterstaat. Thus, the spatial distributions of these sections do not match, although the names of the sections in D-HYDRO suggest that they do.

Figure 11 Roughness estimate trajectories in the main channel of the Waal. The area within the black square is the area of interest, the Midden-Waal. Note that section 2007 has a different roughness formulation due to the fixed layer near Nijmegen. The subdivision within the area of interest is needed to define the three different calibrated roughness heights in the Midden-Waal.

Figure 12 Spatial distribution of calibration factors sections. Note that the section names are not the same as in Figure 11. The calibrated roughness is determined by multiplying the roughness estimate with the calibration factors. The subdivision within the area of interest was needed to calculate the three different calibrated roughness heights in the Midden-Waal.

The differences in the spatial characteristics of the roughness estimation and calibration factor sections forced us to define 3 roughness targets in order to analyse all possible combinations of roughness estimation and calibration factors in the Midden-Waal. Table 1 summarises the parameters based on these spatial characteristics for each of the 3 roughness targets. The spatial distribution of these sections can also be found in Figure 11 and Figure 12.

Table 1 Formula coefficients background roughness and roughness multipliers (Niesten et al., 2022). *The section names in the 2nd and 3rd column correspond with the section names in Figure 11 and Figure 12 respectively.*

Target nr	**Roughness estimate**	**Calibration multiplier**	**Param A,B**	**Cfac Q = [800, 1580,2700] m³/s**
1	2011	2005	0.100 2.5	0.848 0.936 1.001
2	2010	2005	0.083 2.5	0.848 0.936 1.001
3	2010	2004	0.083 2.5	0.854 0.907 0.940

Each of the 3 roughness sections has a roughness estimate defined by parameters A and B, and a discharge dependent calibration factor, which was plugged into equation 3 to determine the calibrated roughness for each of the 3 sections.

Since water depth is the variable in the roughness estimation equation (Eq. 1) and a discharge dependent calibration was performed to obtain the calibrated roughness in the default model, a relationship between water depth and discharge in each of the 3 roughness sections was needed to determine the target main channel roughness. Therefore, D-HYDRO model runs were performed using the default model to obtain a discharge-water depth relationship for each of the three roughness sections mentioned above. The model was run 8 times with steady-state discharges of [575, 800, 1050, 1350, 1550,1850, 2200,2500] m^3/s. The lowest discharge corresponds to the lowest discharge for which bed measurement data were available. The upper limit corresponds to the discharge at which the floodplain begins to be inundated. The discharges in between are chosen randomly, but the interval between discharges was kept ≤ 300 m^3/s to ensure sufficient detail in the Q-h relationship. A smaller discharge interval would not add much value as only main channel discharges were used. In the main channel, the Q-h relationship is a relatively straight line. Once the floodplain starts to be inundated, the Q-h relationship starts to bend more.

The resulting water depths, measured with an observation point in the centre of each of the three roughness sections in the model after 3 days (steady h), were used for the discharge-water depth

relationship in each roughness sections, for which the spatial distribution is shown in Figure 11 and Figure 12.

As in the development of the Rhine Branches model (Niesten et al., 2022), the calibration factors were interpolated in steps of 1 m^3/s over the entire calibrated discharge domain (800 m^3/s – 2500 m^3/s). The same was done for the water depths.

Finally, equation 4 was filled in with the obtained water depths, calibration factors and formula coefficients which can be found in Table 1. With the calibrated roughness values for each of the 3 sections, the determination of the new formula coefficients (Eq. 3) could be started.

2.5.3 Determining new coefficients and influence of discharge history

The determination of the coefficients and length of discharge history period were determined as follows:

- The starting point was to create as uniform a formula as possible for the three sections: the formula coefficients were kept the same for each section, except for 1 coefficient that was allowed to vary to capture the differences in calibrated roughness. Too many free coefficients make it impossible to interpret the formula physically, while the analysis of varying variable is much easier.
- The formula was filled in for the instances where bed measurements were available: 55 bed measurements where the discharge was less than 2500 m^3/s. This resulted in 55 roughness estimates which were optimised. This is described in the next two points.
- The optimal values for the coefficients for A_{new} and B_{new} and $P1$ (see Equation 3) in each of the three roughness sections were determined using the 'differential evolution' function from the optimisation module of the 'SciPy library' in Python. The optimisation objective was to minimise the absolute difference between the formula estimate and the calibrated roughness target (Equation 4). During the optimisation process, each set of coefficients that reduced the absolute difference, compared to the previous optimal value, was stored.
- The optimal and suboptimal values were compared for the three roughness sections to find similarities and large differences. This was used to determine which coefficients were suitable to keep the same in each of the three formulae and which coefficient(s) were suitable to capture the differences between the three roughness sections.
- To determine the length of the discharge history period Q_{hi} , the scarce available literature was used. Zomer et al. (2021) found a median (50th percentile) bedform turnover time of approximately 50 days after the discharge peak in the first weeks of January 2018. The 95th percentile of bedform turnover timescale is approximately 125 days as is illustrated in Figure 13. However, ~25 days has the highest probability. Therefore it can be concluded that the uncertainty is large as the range in days is large. Therefore, the optimization was performed for a discharge history period of 25 days.

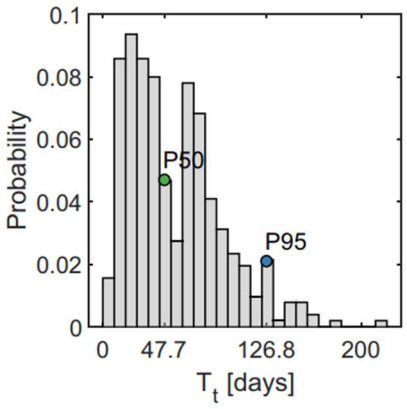

Figure 13 Histogram bedform turnover time (Zomer et al., 2021)

- To analyse the impact of the discharge period, a sensitivity analysis was performed for the following number of days: [5, 25, 50, 75, 100, 125]. This sensitivity analysis was only performed for roughness section 1 (see Figure 11). The optimal parameters for section 1, determined in the steps above were, used. P1, was allowed

to vary freely to analyse the importance of the discharge fraction Q/Q_{hi} for a varying number of days of discharge history.

The quality of the fits was determined using a Normalized Root Mean Squared Error:

$$NRMSE = \frac{\sum \frac{(P-O)^2}{n}}{\max(O) - \min(O)} \quad \text{Eq. 6}$$

Where O are the 'observed' calibrated roughness values in the standard model, while P are the predictions of the new roughness estimation formula. The RMSE is normalised by the range of calibrated roughness values in the standard model.

2.6 RQ 3: Determination and calibration new roughness sections

In this section, the methodology used to analyse the added value of detailed physically based roughness sections to the main channel bed roughness estimate is presented. In the default model, the roughness sections were determined based on the trend in dune height, but this was done on a large scale. The aim of this research question was to analyse whether the calibrated values of the new roughness sections could somehow be related to the bedform characteristics in the new roughness sections.

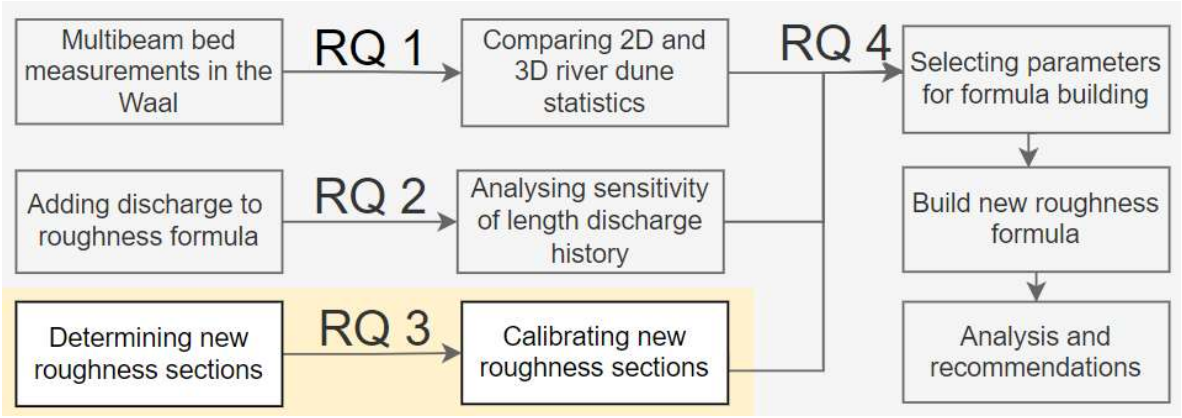

2.6.1 New roughness sections

The spatial trend in mean dune height was used to determine the new roughness sections in the Midden-Waal. This was also done in Niesten et al. (2022), but was now executed on a more detailed scale as suggested by Haase et al. (2023). Because the calibration was to be performed for several discharge levels in the Waal: [800, 1350, 1900 and 2500] m^3/s, the data set of averaged dune heights was divided into 4 discharge ranges, which was done by comparing the dates of the multibeam measurements with the discharge in the Waal at that moment. Since not much bed data was available for the highest discharge range (Figure 14, colours correspond with calibration discharge levels), only the 3 lower ranges were further analysed in this study.

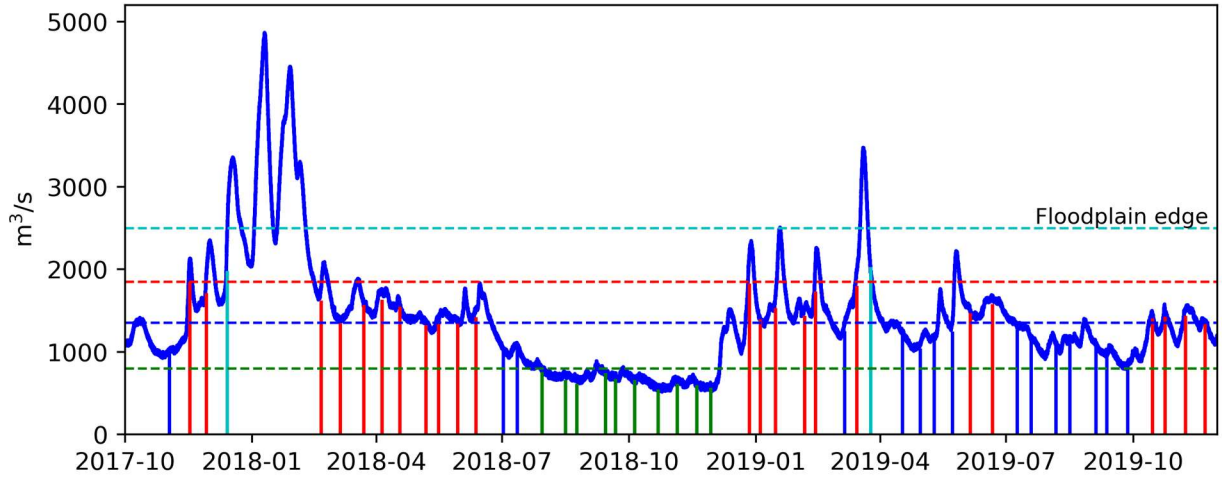

Figure 14 Bed measurement per discharge range which are used for calibration: [800, 1350, 1900 and 2500] m^3/s. For discharges between 1900 and 2500 m^3/s only 2 bed measurements are available which not enough to draw reliable conclusions. Therefore, analysis is restricted to 1900 m^3/s.

The discharge levels for calibration were chosen such that the lowest level (800 m^3/s) corresponds to the lowest discharge for which the default model was calibrated, while the highest discharge level

(2500 m^3/s) corresponds to the discharge in the Waal where the floodplains are not yet inundated. The 2 other levels are chosen in between the upper and lower discharge levels.

The most appropriate number and location of roughness sections was determined by minimising the standard deviation between the section averages and the individual dune height per section of 1 km in the Midden-Waal. The standard deviation was calculated using the following equation:

$$\sigma = \sqrt{\frac{1}{N}\sum(H_i - \bar{H})^2} \qquad \text{Eq. 7}$$

Where H_i is the mean dune height per section of 1 km and $\bar{H}$ is the mean dune height per roughness section. The results of the minimisation and the ideas behind it will become clearer when the visualisations are added and described later in this section.

The final dune height, location and length of the 3 final roughness sections are given in Table 2 & Figure 15. The coloured lines (H_i) in the figure are determined by averaging the dune height in the Midden-Waal over sections of 1 km, which is done every kilometre from the start of the Midden-Waal. For example, at 3 km from the start of the Midden-Waal, the dune heights are averaged over 2.5-3.5 km. The number and lengths of the black lines correspond to the spatial distribution of the 3 proposed roughness sections.
The smaller the variation of the coloured lines around the black lines ($\bar{H}$), the better the spatial variability in dune height is captured by the roughness sections. The minimised standard deviations per discharge range are presented in the right top corner of the subplots in Figure 15.

Table 2 Roughness sections

Section	Interval [km]	Length[km]
1	0-3	3
2	3-11	8
3	11-17	6

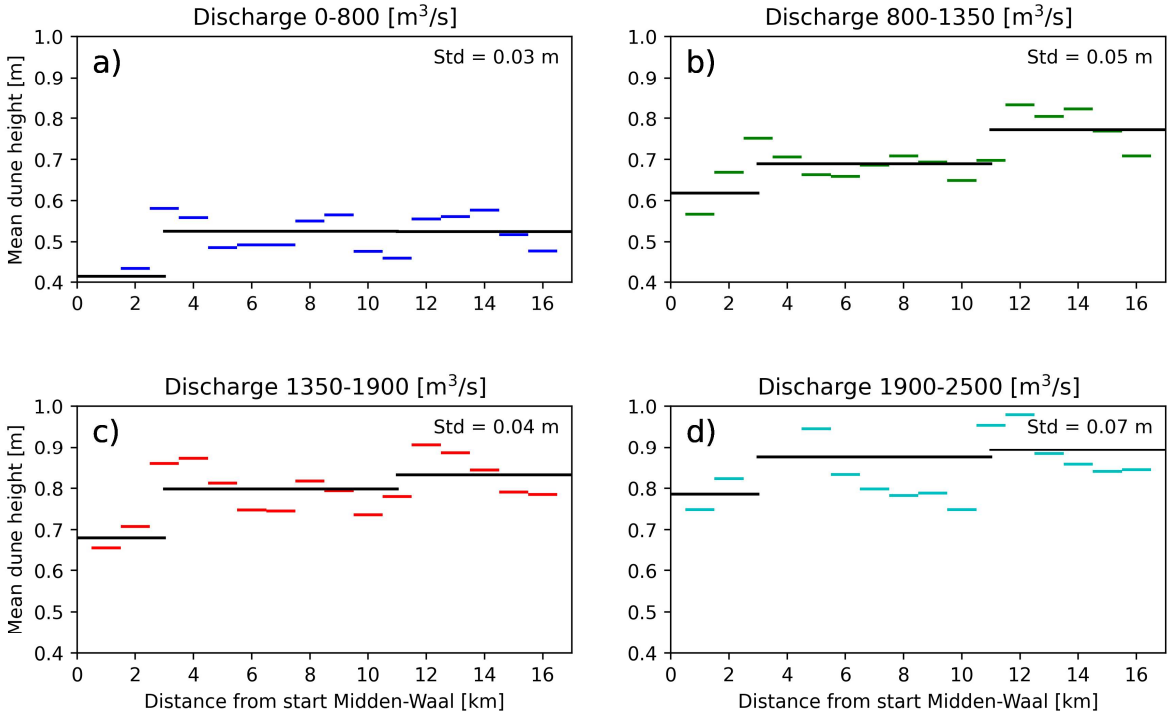

Figure 15 Derivation of new roughness sections in the Midden-Waal. The coloured lines show the averaged dune height over sections of 1 km length (H_i). The black lines are the final roughness sections ($\bar{H}$), based on minimizing the standard deviation of the coloured lines around the black lines.

2.6.2 Calibration new roughness sections

The next step was to calibrate the new roughness section determined in Section 2.6.1. Therefore, roughness sections within the Midden-Waal of the default model (Figure 2 and Figure 12) were modified to new roughness sections, determined based on the trend in dune height in the Midden-Waal, which can be found in Figure 16.

Figure 16 Modified calibration factor sections in the Midden-Waal based on trend in dune height. Roughness outside the Midden-Waal is not modified.

To ensure that the transitions between roughness sections were smooth and did not cause unwanted hydrodynamic effects (abrupt acceleration or deceleration of the flow), the developers of the default model introduced 2 km long transition zones between roughness sections (Niesten et al., 2022). These transition zones were also applied to the new roughness sections in this study, as shown in Figure 17.

Figure 17 Transition zones between roughness sections to ensure smooth hydrodynamic effects. The roughness is interpolated between two adjacent roughness sections over a length of 2 km. The higher the percentage, the higher the contribution of the roughness section on a part of the river. Transition zones are shown for sections 1 and 3.

The final step was to select discharge periods for each of the 4 discharge levels for which the recalibration would be performed: [800, 1350, 1900, 2500] m^3/s. The main channel roughness in the existing Rhine Branches model is discharge dependent:

- The model determines the roughness estimate based on Equation 2. Function of the water depth
- This roughness estimate is then multiplied by the discharge dependent calibration factor to determine the final main channel roughness height (k_s), which results in figures such as Figure 1. See also Equation 4 for the formula to determine the calibrated roughness.

Discharge periods were selected for the four calibrated discharge levels. Figure 14 shows the discharge time series used to calibrate the four discharge levels in panels b-e. The lengths of the discharge periods are comparable to those used in the default model: ~6 days (Niesten et al., 2022). The moments are chosen so that the discharge barely exceeds the discharge level for which the calibration was performed. This is because the calibration is performed from low to high discharge levels. As mentioned above, the model interpolates calibration factors between the four discharge levels. The uncalibration factors for each of the discharge levels have a default value of 1, so if the discharge time series exceeds the level for which it is calibrated, the model will interpolate using an uncalibrated higher discharge level, affecting the calibration results.

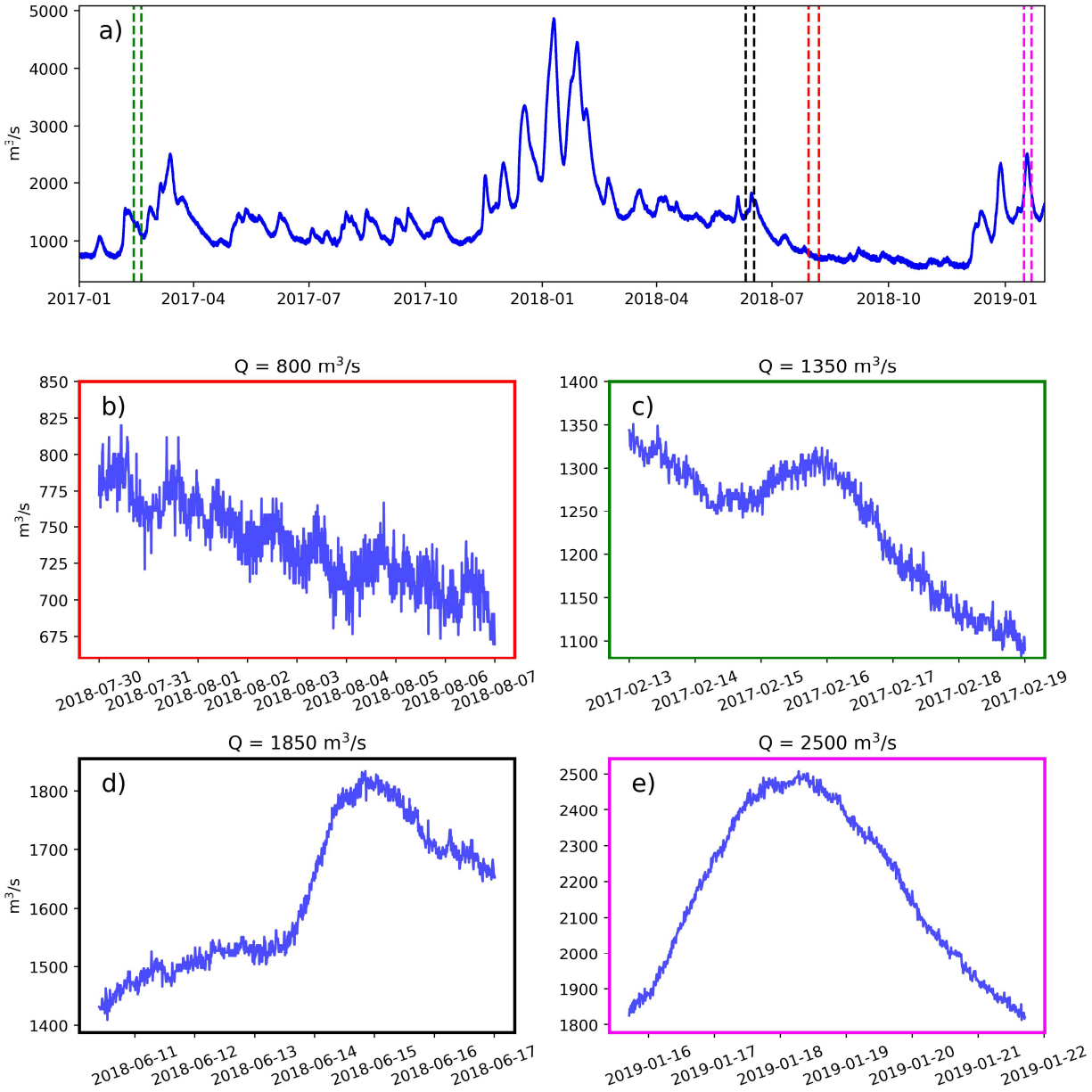

Figure 18 Discharge timeseries used for calibration. Calibration is performed to determine calibration coefficients for Q = [800, 1350, 1850 , 2500] m^3/s. Therefore, these values are also approximately the maximum in each of the timeseries

The calibration was performed using OpenDa, an open interface of tools that can be used for data assimilation and calibration of numerical models. OpenDa required observed water level time series as input for comparison with model output. Water levels at the upstream edges of sections 1, 2, 3 and 2004 (see Figure 16) were used as reference for comparison with model output. Section 2004 was also recalibrated as only part of this section remained intact after the Midden-Waal was cut into three roughness sections. The set of calibrated discharge-dependent roughness multipliers for reach 2006 was not recalibrated as no changes were made to this reach.

For the calibration of the whole Rhine Branches model, the calibration sections in the Waal corresponded to the trajectories between the LMW gauging stations. However, this was no longer the case after the Midden-Waal was divided into three sections. Therefore, stage relation curves

were used to determine the water level at the upstream edges of each of the 4 recalibrated roughness sections.

The 4 discharge dependent calibration multipliers at the 4 recalibrated roughness sections were calibrated by running the OpenDa software 4 times (for the discharge 4 discharge levels which are calibrated separately), starting with the lowest discharge level, 800 m3/s. The stop criterion was set at 2 cm for each observation point. 1 cm did not appear to be feasible. More detailed calibration settings can be found in Appendix A, Figure 28.

2.7 RQ 4: Establishment final formula

For the final research question, section, all the findings from the previous research questions were combined to produce a final roughness formula.

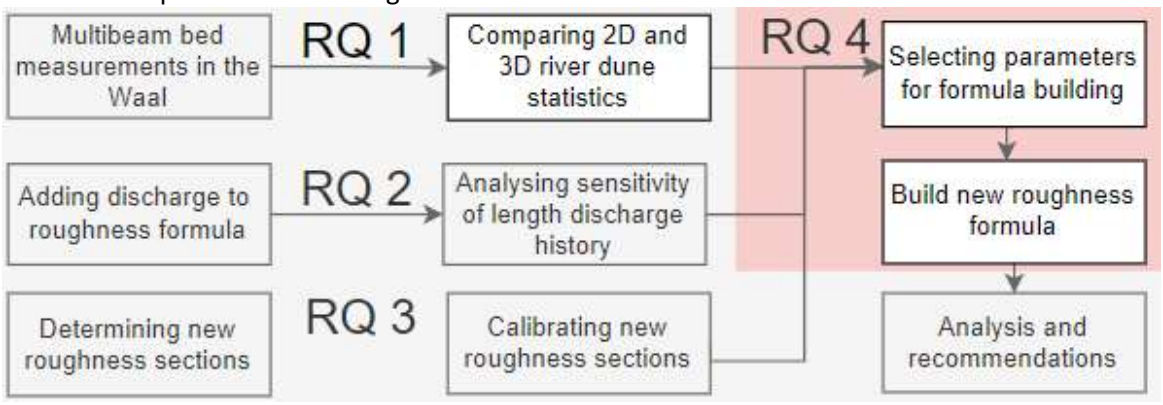

Only those parts that clearly improved the roughness estimate were included. This means that:

1. Either 2D or 3D dune statistics are used,
2. Discharge history was included, or not,
3. The new formula would be established for the new roughness sections, determined in section 2.5, or the roughness sections of the default model, used in section 2.4.

As in section 2.3, the roughness target is defined as:

$$\boldsymbol{k_{s\,target} = Ah^{0.7}\left(1 - e^{-Bh^{-0.3}}\right) \times \left(C_{fac}\right)^{6}} \qquad \text{EQ. 8}$$

The variables in this formula were explained before. Possible inputs to the new formula are Q, Q_{histo} $, H, L$ or other relevant variables found during the analysis. The procedure for setting up the formula was the same as in Section 2.5. However, now probably with more variables if there was reason to do so. Again, the aim was to produce a roughness estimate that was as close as possible to the calibrated roughness, the roughness target for each of the three roughness sections. To this end, a sensitivity analysis was done with the relevant variables found during the research, to determine which variables and wherein the final roughness estimate formula (in the exponent (like B in equation 8, or as a multiplication term, like A in equation 8, or both). In this way, the variables with the most added value were identified.

3. Results

This chapter presents the results of the analysis of the:

1. Comparison of 2D dune parameters with the derived 3D bedform parameters.
2. Influence of discharge history on the degree of required calibration.
3. Recalibration of the Midden-Waal using new roughness sections based on trend in dune height.
4. The establishment of the final roughness formula based on the results of the first 3 research questions

3.1 RQ 1: 2D dune vs 3D bedform statistics

The goal of RQ 1 was to determine whether 3D dune statistics would add value to the current 2D approach.
Figure 15 shows the results of the comparison between 2D and 3D dune statistics for 2 locations along the Midden-Waal. These locations were chosen because they appeared to be representative of the other locations within the Midden-Waal. Each scatter point represents a point in time when the bed measurements were taken.
The results are presented for each of the three panels (a-c)

a. The mean dune heights in 2D and 3D are positively correlated, with little scatter around the linear fit. Thus, the 3D approach defines the dune height in a similiar trend as the 2D approach.
   However, the 3D dunes appear to be higher than the 2D dunes as they are above the black $y = x$ line. This means that either this 3D approach overestimates the dune height, or the 2D approach underestimates the dune height, or a combination of both.
   This difference in height may be caused by the way how height is defined. In the 2D approach, dune height is defined as the height of a dune crest above the next trough (Lokin et al., 2022), whereas in the 3D approach, the difference between the elevation of the peaks and the 15^{th} percentile of the bed elevation in the analysed sections was used as the height definition.
   The 3D dunes are higher at the 3 km chainage than 5 km further downstream. However, the highest 2D dunes are found at chainage is 8 km. However, most of the 20 highest 2D dunes are at chainage 3 km. This shows that there is no clear spatial consistency between 2D and 3D dune height.
b. The next panel compares the 2D dune length with the 3D dune size. Comparing two different quantities is not fair, but it might give us some insights, as dune height - size combinations might reveal some roughness sources that are not covered in 2D by using a length only.
   It is noticeable that the green line is almost horizontal, so the 3D size does not increase much with the 2D length at 8 km chainage, while the blue lines show that the 3D size increases with the 2D length at 3 km chainage. Again, this may be due to the way the 3D statistics were derived: for the dune size, a fixed percentile was used to determine the size.
   Finally, there is a lot of scatter in the blue dots, which shows that, by chance, larger dunes are identified at 3 km chainage than at 8 km chainage. In addition to the methodology, an explanation for this scatter could be that the bed development is site-specific. It can be concluded that the 3D dune size does not (yet) give practical results.
c. The third panel shows the comparison between the 3D dune length and the 2D dune length. The first thing that stands out is that the y=x line is almost out of the picture, showing that the 3D dunes are much shorter than the 2D dunes (using the same axis here would lead to

illegibility). This is logical because the 3D length is the average length over the whole 3D dune, rather than using a single length from trough to trough. In the 2D approach, the trough after a crest is a starting point for the next dune, whereas in the 3D approach the dunes are not directly adjacent, as can be seen in Figure 10.
As with dune height, the 2D dune length follows the same trend as the 3D dune length. However, the slope of the dune height fits is close to 1, while the 3D dune length does not increase as quickly.
There is a lot of scatter in the blue dots, showing that the 3D approach identifies long dunes, while they are not as long in the 2D approach.

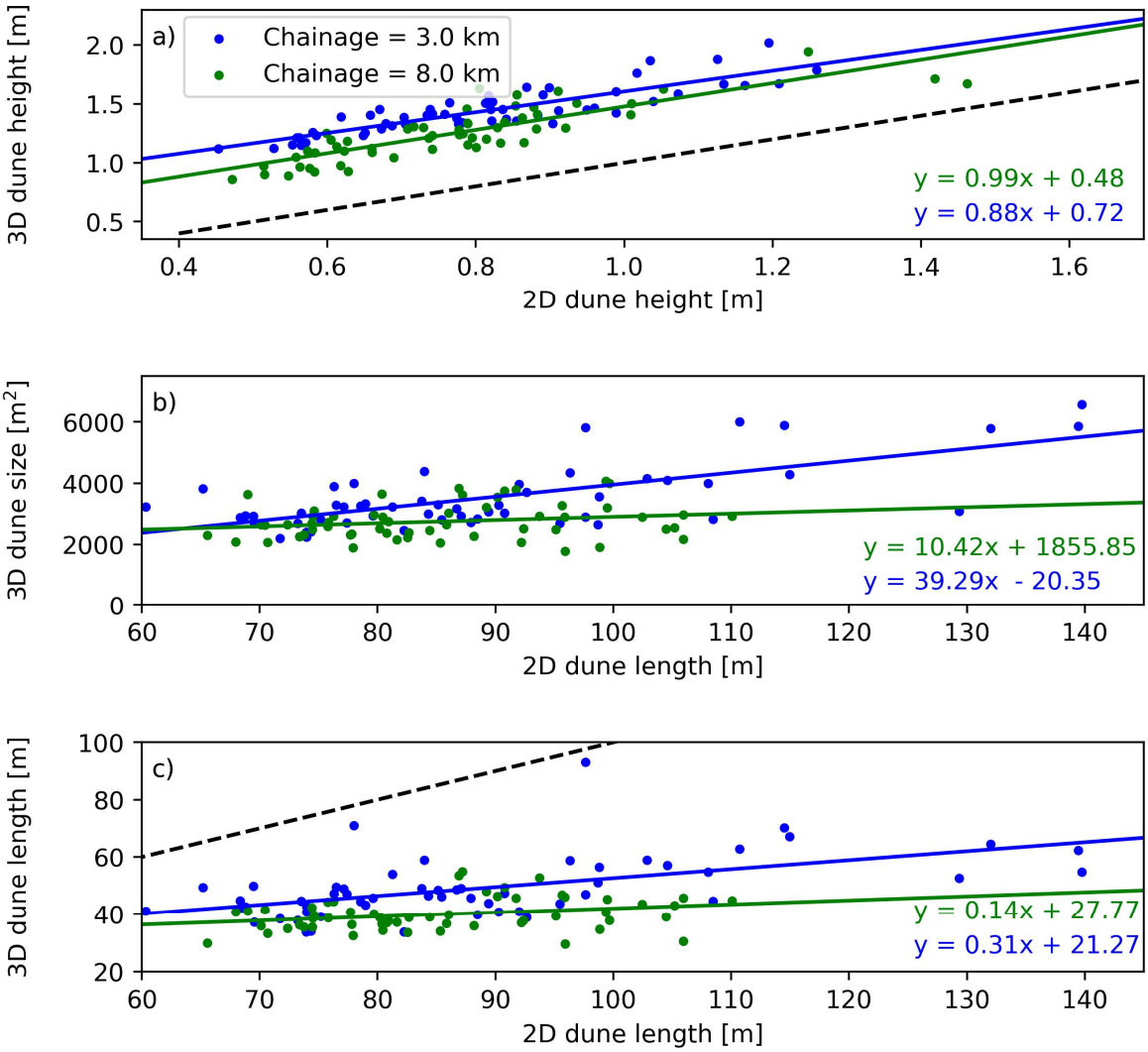

Figure 19 Comparison of 2D vs 3D dune statistics. This is done for 2 locations within the Midden-Waal. The black line is the 1:1 line. The formula variables correspond to the variables on the x and y axis.

Thus, 3D dunes differ more from 2D dunes in length than in height. This difference is mainly due to the way the 3D statistics were derived. The analysis showed some spatial differences in bed development, but this could also be concluded from the analysis of the 2D dune statistics. In addition, 3D size, which was the most innovative statistic here, did not give any useful results. Therefore, the use of 3D dune statistics has no added value (yet). The 2D dune statistics will be used further in this research.

3.2 RQ 2: Discharge history

The aim of this research question was to determine whether the addition of discharge history to the roughness estimation formula would reduce the degree of calibration required.
The first part of this research question was to determine the formula coefficients for the new roughness estimation equation. These are presented first. The quality of the new roughness estimates is then described. The trends of the 2D dune statistics in the new roughness estimate are then analysed as they may have added value later in this research. Finally, the results of the sensitivity to the length of the discharge history are presented.

Figure 20, Figure 30 and Figure 31 (the last two can be found in Appendix B), corresponding to roughness section 1, 2 and 3, show:

1. 4 subplots with the same lines and scatter points. However, each subplot shows a 2D dune statistic, or the value of discharge fraction Q/Q_{his}. The colour bar next to each subplot shows the values of the statistic shown.
2. Coloured scatter: the new roughness estimate by the new formula.
3. In blue: the calibrated roughness in the default model.
4. In black: the roughness estimate from the default model

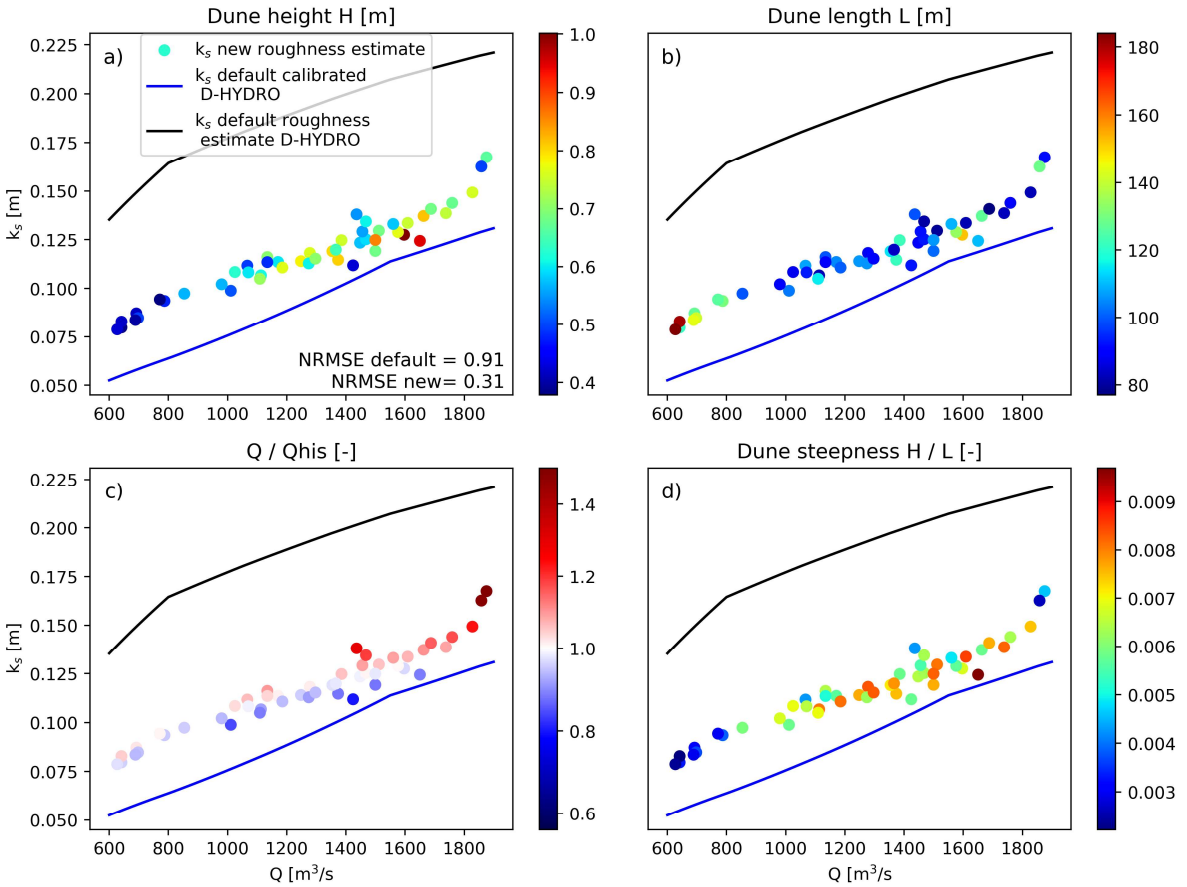

Figure 20 New roughness formula for section 1. Existing formula (Equation 2) is extended with the discharge fraction $Q/Qhis$. The colour scale in the scatter shows the values of 3 dune statistics and the discharge fraction $Q/Qhis$.

3.2.1 Formula coefficients

The new roughness estimates were obtained by optimizing the coefficients in Eq. 9. Eq. 10 shows the optimal coefficients for coefficients for the new roughness estimate in section 1 can be found in the following equation. The other two formula can be found in Appendix A.

$$k_{s\,new} = A_{new}\left(\frac{Q}{Q_{his}}\right)^{P1} h^{0.7}(1-\exp(-B_{new}\,h^{-0.3}) \quad \text{Eq. 9}$$

$$k_{s\,new} = 0.04\left(\frac{Q}{Q_{his}}\right)^{-0.11} h^{0.7}(1-\exp(-25\,h^{-0.3}) \quad \text{Eq. 10}$$

It was decided to allow the parameter P1 to vary freely as the other coefficients appeared to have relatively similar values. The values for P1 are -0.11, 0.35 and 0.28 for sections 1-3 respectively. This shows that the added value of the discharge history is small for section 1. This is probability due to the fixed coefficients in the formula. A lower value for A_{new} might have improved the quality of the fit, accompanied by higher value for P1, but this was not part of this research question.

3.2.2 Quality of the fit

Figure 20 shows that the new roughness estimate is closer to the calibrated roughness (blue) compared to the default roughness estimate in D-HYDRO, which means that the new roughness formula is an improvement over the default formula as less calibration is needed to coincide with the calibrated roughness in the default model. The same applies for the estimates in the two other sections (Figure 30 and Figure 31).

This can also be quantified. The quality of the fit is determined by a Normalised Root Mean Square Error (NRMSE). Table 3 shows the NRMSE of the standard roughness estimate and the new roughness estimate for all three roughness sections. The higher the NRMSE, the more the roughness estimates deviate from the calibrated roughness in the default model.

Table 3 Normalized RMSE for default roughness estimate and new roughness estimate for the 3 sections

Section	NRMSE default estimate	NRMSE new estimate
1	0.94	0.30
2	1.02	0.17
3	1.50	0.22

The NRMSE has decreased for all new roughness estimates, showing that the discharge history has added value to the roughness estimate. The estimates in section 1 deviate the most from the calibrated roughness: on average 30% of the range of actual values, showing that a perfect fit cannot be obtained by using discharge history and updated formula coefficients alone.

3.2.3 2D dune and discharge history statistics

In addition to the performance of the new roughness estimation formula, Figure 20 also shows the dune statistics $(H, L, H/L)$ and the discharge fraction $(Q/Qhis)$. The following bullet points correspond with the subplot names in Figure 20:

a. As expected from the literature (Warmink, 2014; Bradley & Venditti, 2017; Lokin et al., 2022), dune height increases with discharge. There are some exceptions around 1450 and 1850 m^3/s (dark blue points), but these bed measurements were taken relatively quickly after the long low flow in the last months of 2018 (see Figure 8). The bed measurements around 1600 m^3/s that show a high dune height are the results of bed measurements during and just after the high discharges in the first months of 2018 (see Figure 8). It can be concluded that discharge history is from great importance in the dune height – discharge relation.

b. In line with Lokin et al. (2022) dune length decreases with increasing discharge. The dune length also have some outliers related to discharge history. As with the dune height, it can be concluded that parametrising dune dimensions as function of the water depth alone does not capture discharge history related dune dimensions.
c. The $Q/Qhis$ uses a discharge history length of 25 days. Figure 20 shows little scatter, while the discharge fraction values differ. This is probably due to the power, close to 0. This is different for the roughness estimates shown in Figure 30 and Figure 31 in the Appendix. Here it can be seen that the roughness estimate increases with a larger value for $Q/Qhis$. This shows that the 25 days of discharge history does not have much added value in this context, but using only the discharge may be appropriate as well. The two figures in Appendix B give raise the thought that a combination of $Q/Qhis$ and H/L may have an added value as these fractions seem to be negatively correlated.
d. Dune steepness (H/L) follows approximately the same colour trend as dune height. Dune length (which does not adapt to flow conditions as quickly as dune height (Warmink, 2011)) slightly alters the colour trend. Including actual dune dynamics in the roughness estimate would increase the physical nature of the formula. The dune steepness was included in the roughness estimate Van Rijn, (1984), which shows that the addition of this term is not random. The advantage, as with the discharge history fraction $Q/Qhis$, is that this parameter is dimensionless.

3.2.4 Sensitivity discharge history period

Figure 21 shows the performance of the formula when the number of discharge history days is varied during optimisation. As in the previous section, P1 was allowed to vary freely:

$$k_{s\,new} = 0.04\left(\frac{Q}{Q_{his}}\right)^{P1} h^{0.7}(1-\exp(-25\,h^{-0.3}) \qquad \text{Eq. 11}$$

Each subplot shows the Normalized RMSE and the optimised value for P1. As seen earlier in this section, the outcomes of the new roughness estimate (Eq 11) are scattered, while the default calibrated roughness and roughness estimate in D-HYDRO correspond to the blue and black linen respectively.

Comparing the NRMSE, it can be seen that a discharge period of about 50 days has the best fit, with a NRMSE of only 0.13. P1 here is 0.23 here, showing that the contribution of the discharge fraction $Q/Qhis$ is has a more positive effect on the quality of the fit compared usable compared to other discharge periods. Longer discharge history periods have a slightly higher NRMSE, but the contribution of the discharge fraction is limited by the low value of P1, which forces the contribution of the fraction closer to 1.
What stands out is that the slope of the default calibrated roughness is different from the slope of the imaginary fit through the scatter, indicating that the inclusion discharge history alone does not capture the trend in roughness. This may not result in large calibration factors in the discharge domain assessed in this research <2500, but when the imaginary fit through the scatter points is extrapolated, the new roughness estimate may deviate more.

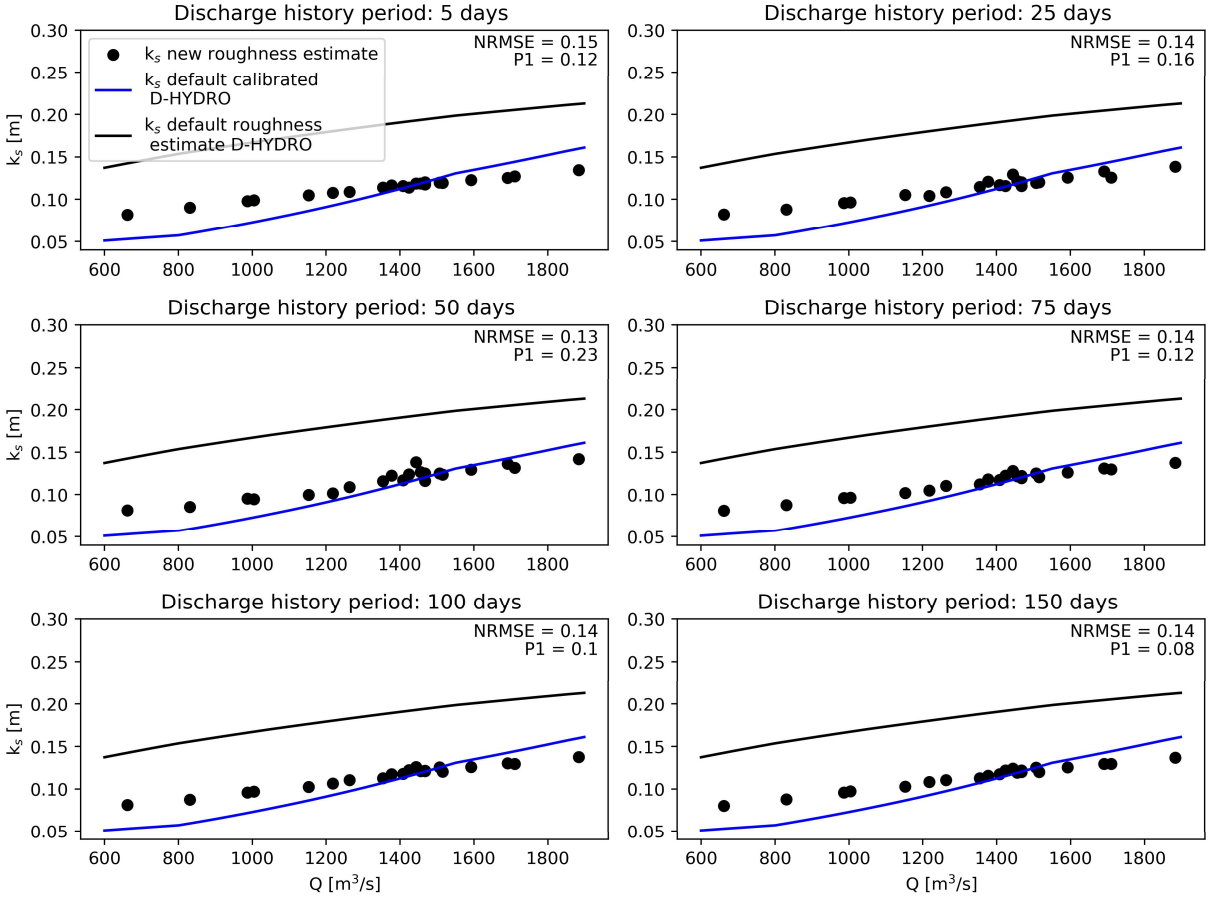

Figure 21 Senstivitiy analysis discharge period. For each subplot, the RMSE and the optimal value of P1 is shown.

3.3 Calibration of new roughness sections

The aim of this research question was to determine whether new roughness sections based on the trend in dune height in the Midden-Waal would lead to new insights into the relationship between bed geometry and calibrated roughness.

3.3.1 Final roughness

This section presents the results of the calibration of the 3 new roughness sections. Table 3 shows the calibration multipliers resulting from the OpenDA calibration. The calibration multipliers vary for each section. The range of calibration factors is largest for the 3rd section, namely 0.249 (0.838 - 1.087).

Table 4 New calibration factors for each discharge level per new section

Section	L1	L2	M1	M2
1	0.907	0.982	0.962	1.005
2	0.836	0.994	0.923	1.011
3	0.838	1.087	0.948	1.003

Figure 18 shows the calibrated roughness for the new roughness sections in colour. The black lines show the calibrated roughness in the standard model. The spatial distribution of the roughness sections is shown in Figure 12 and Figure 16. The main difference between the new calibrated roughness and the default calibrated roughness is the smoothness of the roughness functions. The default roughness is relatively smooth in the evaluated discharge range (<2500 m3/s). The bumpiness of the roughness functions could have been expected based on the new calibration factors. However, the differences per section appear to be marginal. The effect of the 6th power in equation 4 is clearly visible as the bumpiness is extreme, especially around 1350 m3/s. It is noteworthy that the roughness peaks at each of these three sections.

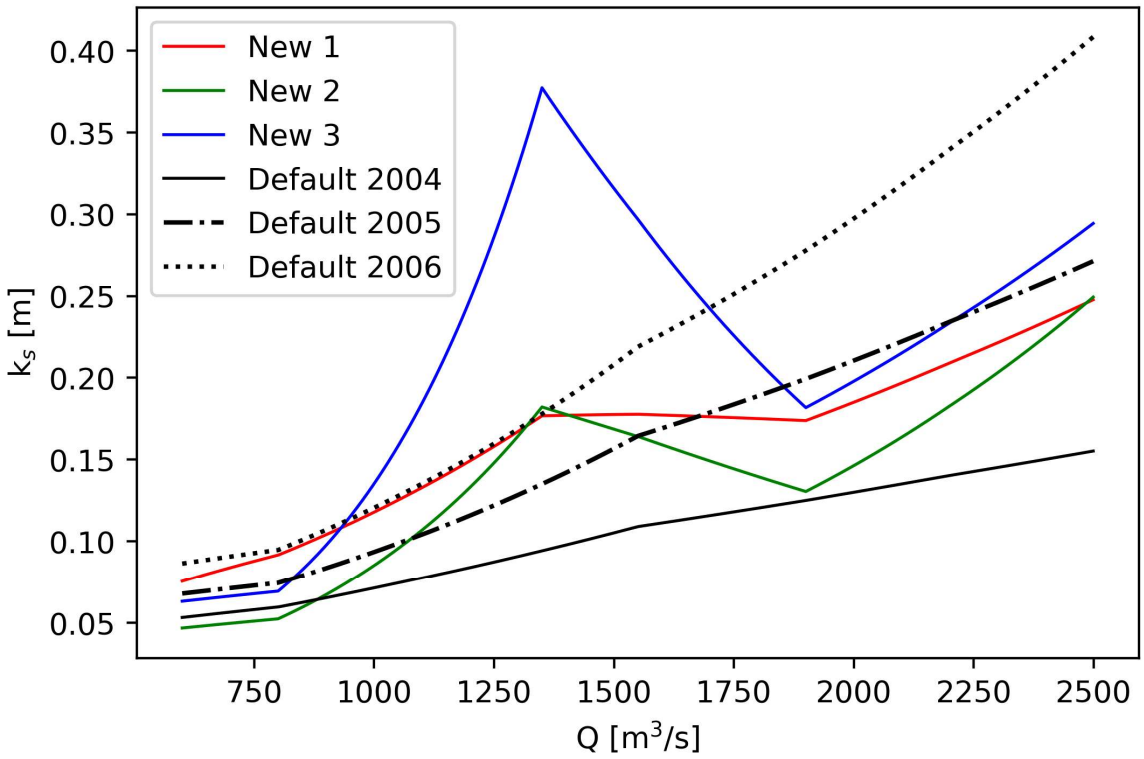

Figure 22 Calibrated roughness, based on Equation 3. The coloured lines are the functions of the new roughness section. The black lines show roughness in the reference situation, the default model.

There are several factors that could have influenced these peaks.

1. Discharge history. Looking at the discharge time series used to calibrate L2 (see Figure 18), the calibration period is preceded by a small peak which is preceded by a short period of low flow. Hysteresis in dune dimensions could have resulted in high and short dunes, meaning that the actual roughness at this time would have been higher than expected. Unfortunately there were no bed measurements available to check this. Therefore, 2 comparable situations, 2 bed measurements just after a discharge peak were analysed (using Figure 16 and discharge time series). However, neither the dune height nor the ratio of dune height to dune length could be related to the peak in the calibration factor.
2. Discharge dependent influence of geometry and other sources of roughness: At low flows, most of the flow passes through the main channel between the groynes. However, as the discharge increases to 1350 m3/s, the contact surface of the water with the river bed increases and the groynes become more pronounced roughness elements. This is also shown in Figure 23. Panel a shows the geometry of a snapshot from the Waal. At lower discharges (panel b), the groynes are barely submerged, whereas at higher discharges (panel c) the groynes become more submerged. the roughness may be reduced.

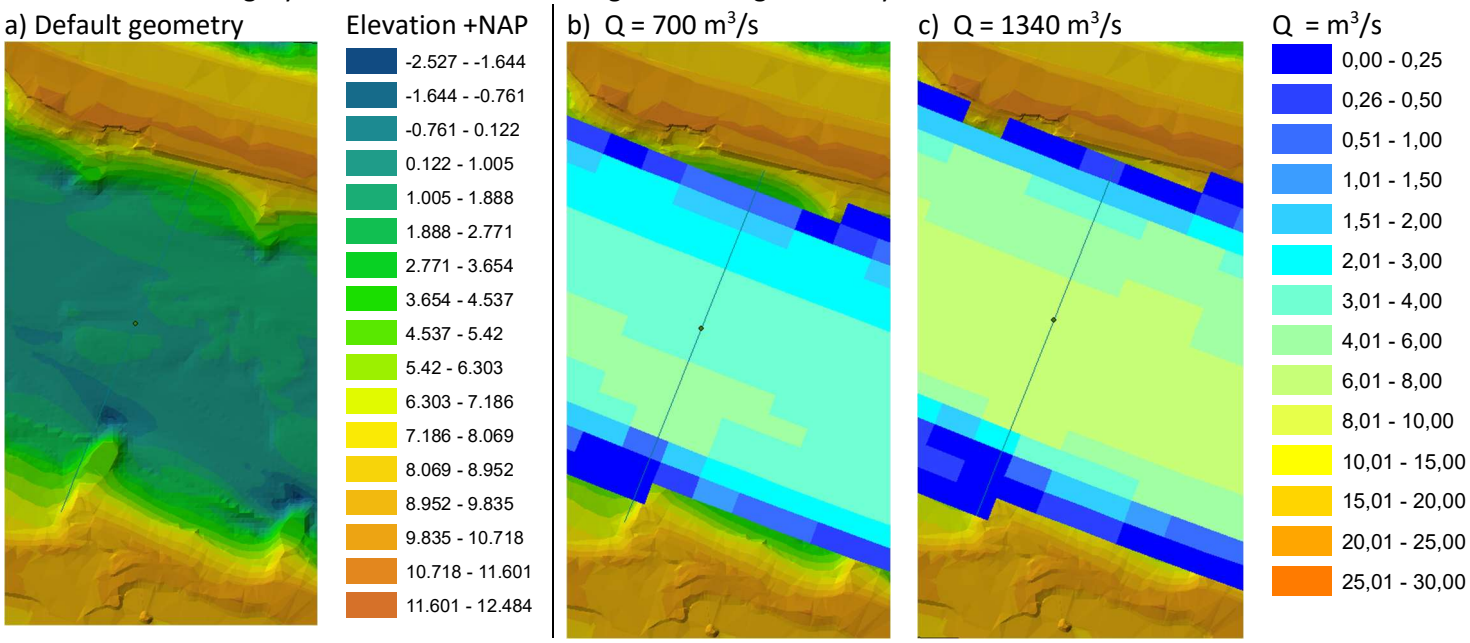

Figure 23 Panel a shows a snapshot of the Waal. Panel b and c show the specific discharges for this snapshot during low and high discharge.

3. The calibration was performed for discharge levels compared to the default calibration. The calibration in this study was performed for [800, 1350, 1900, 2500] m^3/s, while the calibration in the default model was performed for [800, 1580, 2700] m^3/s. The discharge period for the default model calibration was chosen such that 1350 m^3/s was never part of the calibration, which may explain that possible roughness jumps are not well captured in the default calibration.
   Domhof et al. (2018) also investigated an increased number of discharge levels. This study showed that jumps in roughness are common. However, since the roughness in his study is the Manning coefficient n, the comparison cannot be made in much detail, as the Strickler roughness height k_s is much more pronounced compared to a Manning coefficient due to the 6th power in the Manning Strickler conversion (Eq. 5). The study was carried out using discharge and geometry data from 2011 or earlier. The Room for the River projects have changed the geometry of the river and also changed the water levels locally (Berends, 2019).

Therefore, it is difficult to draw conclusions about the correctness of the calibration of the new roughness sections.

3.3.2 Spatial trend roughness vs dune height

The aim of this research question was to look for relationships between the calibrated roughness and the bed characteristics.
The three roughness sections were determined using the spatial trend in dune height shown in Figure 15. This figure shows that the dune height was highest for all discharge ranges in section 3, except for the lowest discharges. Section 1 always has the lowest dune height. Section 2 exceeds section 3 only in the lowest flow range. Comparing this spatial trend with Figure 18, it can be seen that there is no clear relationship between the choice of reach and the final roughness values. Section 3 is always higher than the other two sections, except in the lowest flow range, but since the mutual relationship between sections 1 and 2 does not correspond to the spatial trend in dune height, no relationship can be observed. This means that there are more sources of roughness influencing the main channel roughness in addition to the influence of the main channel bed.

It can be concluded that the 3 new roughness sections do not provide new insights into the roughness-bed relationship due to the uncertainty about the causes of the roughness peaks: the final roughness does not follow the spatial trend of dune height along the Midden-Waal. Therefore, the standard roughness sections and standard calibrated values will be used for the rest of this research.

3.4 RQ 4: Final roughness estimate

In this research question, the results of the previous research questions were combined to produce a final roughness estimate. The following results were used:

1. 2D dune parametrisation is more appropriate than 3D. Dune steepness H/L is a dimensionless parameter that has added value.
2. Discharge history reduces the NRMSE and therefore has had added value in the final roughness estimate
3. The default roughness sections and default calibrated values are not improved by calibrating of new roughness sections, so the default sections are used.

3.4.1 Parameters in final roughness formula

To determine which variables to include in the final roughness estimate formula, the contribution of different terms was determined based on the Normalised RMSE, as shown in Table 5. The contribution analysis was only carried out for section 2, as the lowest NRMSE values were obtained in this section. Note that the presented NRMSE are a result of complete freedom of the coefficients. Restrictions will be used later on in this section.

The first row of the table shows the NRMSE of the roughness estimate in the default model, which is quite high for a normalised RMSE. The next rows show possible formula inputs based on the results of this research are shown. The colours in the 2nd column indicate where in EQ. 12 the variables are included before optimization. The powers in the equation are also of the optimization as well and regulate the relative influence of the discharge fraction $Q/Qhis$ and dune steepness H/L.

$$A_{new} \times (\dots)^{P1} \times h^{0.7}(1 - \exp(-B_{new} \times (\dots)^{P2} \times h^{-0.3}) \qquad \text{Eq. 12}$$

The lower NRMSE of 0.163 shows that the optimised values for the A_{new} and B_{new} coefficients significantly improve the quality of the new roughness estimate. The runoff history in the first part of the equation does not improve the quality of the fit much compared to the new coefficients A_{new} and B_{new}. The dune steepness in the first part of the equation shows a large reduction in the NRMSE, while the reduction in the NRMSE in the second part of the equation due to the dune steepness is slightly less. The added value of discharge history in both parts of the equation is marginal, but the combination of dune steepness and discharge history shows that the NRMSE is reduced by more than 50% compared to the situation where only 2 coefficients were added. This shows that the combination of discharge history and dune steepness are mutually reinforcing and result in a high quality fit.

Table 5 Contribution of formula terms in section 1

Formula variables		NRMSE Section 1
Default D-HYDRO		1.270
A_{new} B_{new}		0.163
A_{new} B_{new} + $Q_{his\ 50\ days}$		0.151
A_{new} B_{new} + $Q_{his\ 50\ days}$		0.162
A_{new} B_{new} + H/L		0.099
A_{new} B_{new} + H/L + Q_{his}		0.083
A_{new} B_{new} + H/L + Q_{his}		0.113
A_{new} B_{new} + H/L		0.121
A_{new} B_{new} + H/L		0.098
A_{new} B_{new} + $Q_{his\ 50\ days}$		0.148
A_{new} B_{new} + $Q_{his\ 50\ days}$ + H/L		0.073

3.4.2 Final roughness formulas

Both the dune steepness and discharge history term in front of the equation and in the exponent have added value. The following equation is the final roughness estimate for section 1:

$$1.02\left(\frac{Q}{Q_{his}}\right)^{0.33}\left(\frac{H}{L}\right)^{0.69}h^{0.7}\left(1-\exp\left(-6.2\left(\frac{H}{L}\right)^{-2.31}\left(\frac{Q}{Q_{his}}\right)^{-0.15}h^{-0.3}\right)\right) \quad \text{EQ. 13}$$

The two equations for the other two roughness sections have the same formula except for the coefficients in front of the equation. The value of these coefficients per equation is given in Table 6. The contribution of the discharge history in the exponent is the lowest, due to the power close to 0. This shows that this term could be omitted, resulting in a clearer formula, but also a fit of slightly lower quality. The quality of the fits is much improved for all 3 sections, showing that the addition of discharge history and dune steepness adds a lot of value. The NRMSE shows that in the worst case the prediction error from the calibrated roughness is 19.2%, which is low compared to the 127% prediction error in the default model.

Table 6 Summary formula per roughness section

	Section 1	Section 2	Sections 3
Free coefficient [-]	1.02	1.04	1.16
NRMSE [m]	0.192	0.083	0.090

Figures 24, 25 and 26 show the scatter plot of these three formulae for each of the three roughness sections. The significance of the four sub-plots has already been explained in Section 2.3. It is noticeable that the scatter is greatest for section 1. This is because the formula coefficients were mainly based on sections 2 and 3 (the calibration factors were the same here, resulting in approximately the same shape, but the default roughness estimate was different in these two sections). The NRMSE could have been reduced by allowing more than 1 coefficient to vary freely. The colour distribution in panels c and d in these figures is shown:

1. More randomised colour distribution in the discharge history scatter compared to Figure 20 in Section 3.2 where only the discharge history was used in the roughness estimation formula. This can be related to:
2. Less randomised colour scatter in the dune steepness scatter, showing that adding discharge history improves the discharge-dune steepness relationship by including the effects of discharge history dependent bed development. This is also evident in panels a and b, where the colour distribution has become more uniform compared to Figure 20 in Section 2.3.

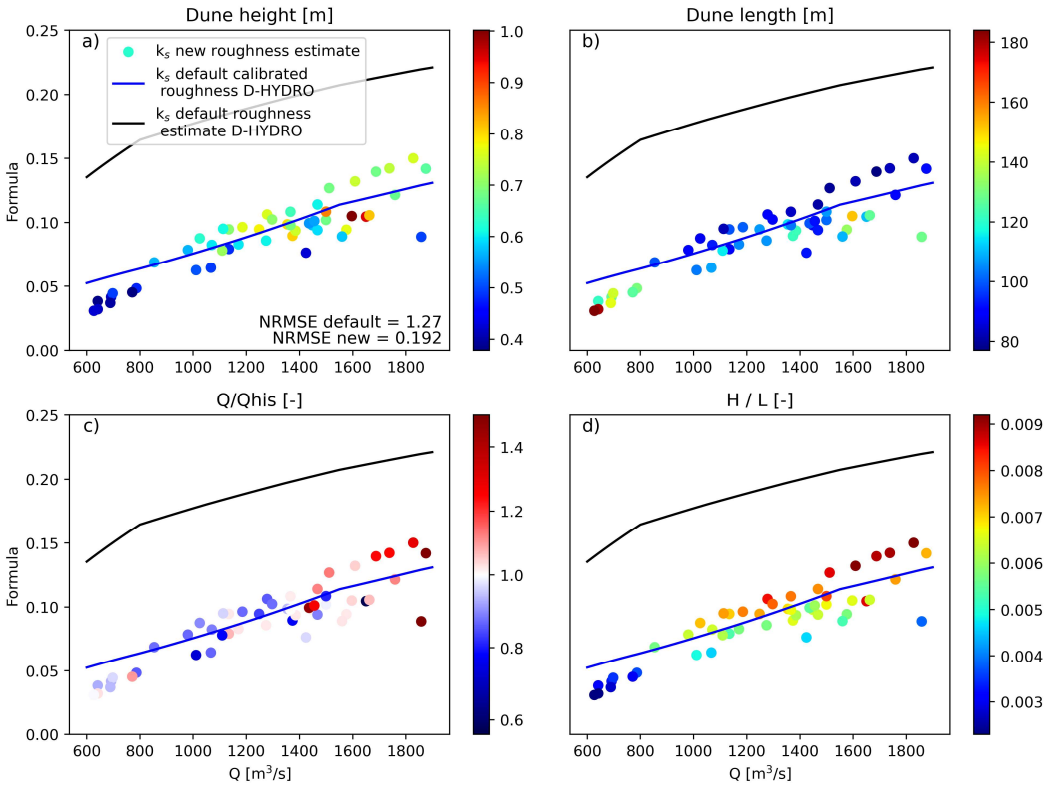

Figure 24 Final formula section 1. Subplots show the 2D dune statistics and discharge history fraction.

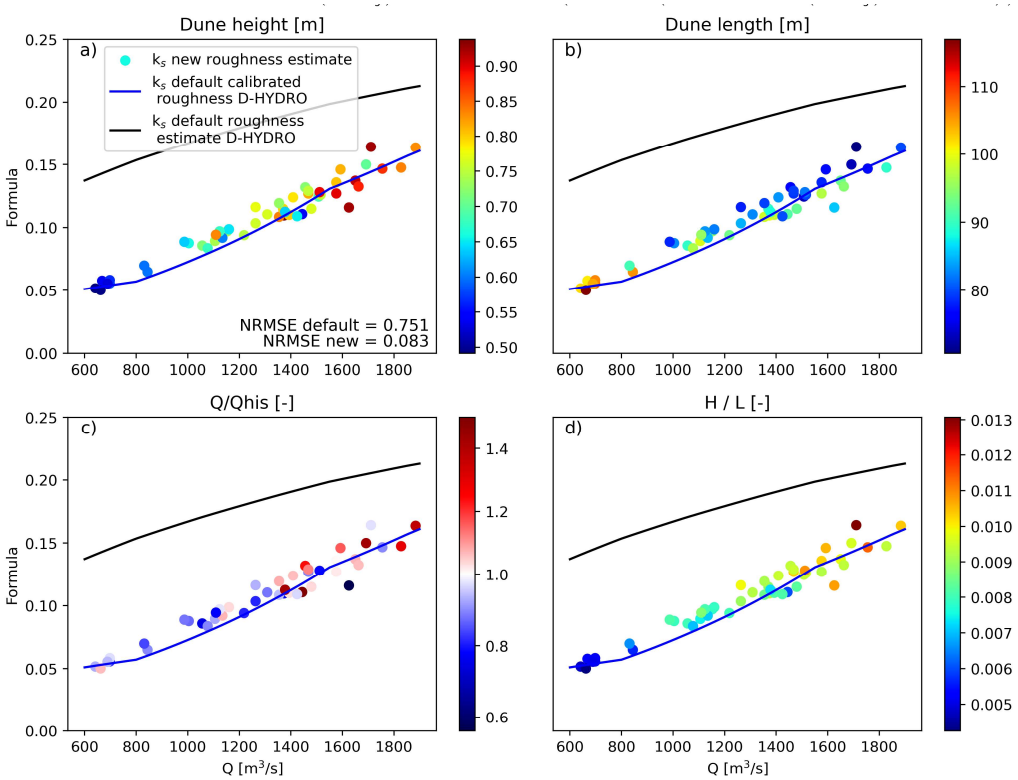

Figure 25 Final formula section 2

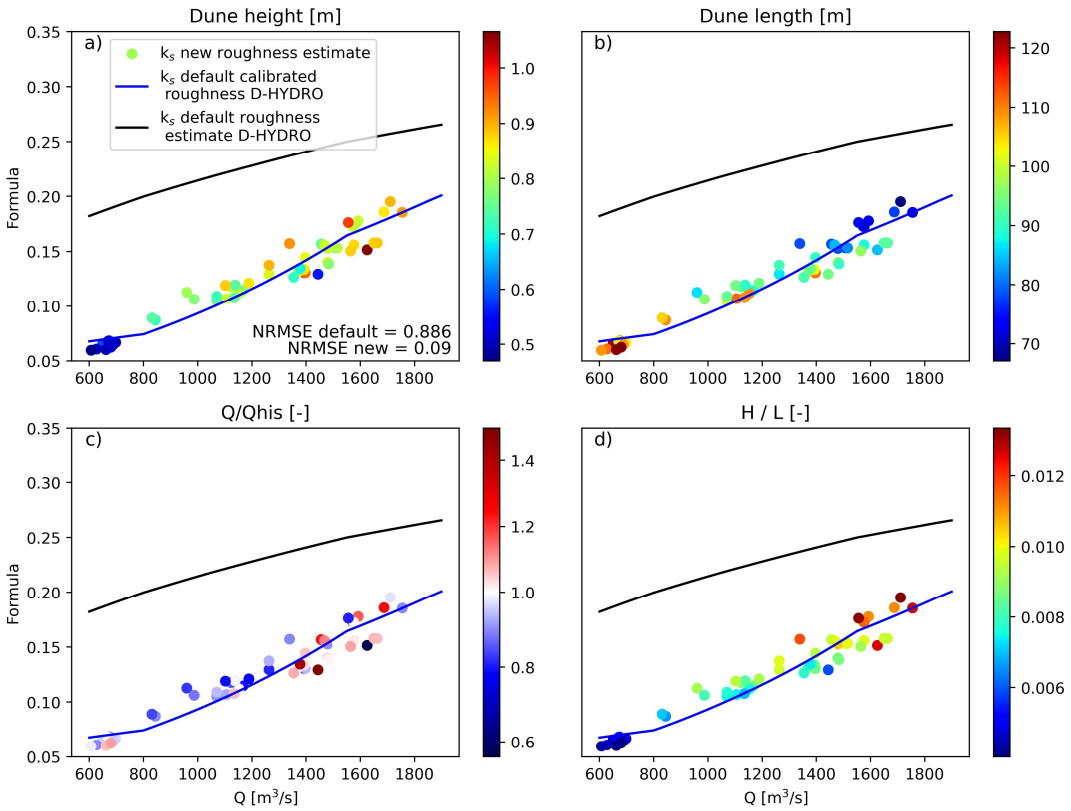

Figure 26 Final formula section 3

3.4.3 Physical nature of formula parameters

Several terms are added to the simplified Van Rijn formula. Better fits have been obtained, with significant decreases in the NRMSE. What is the contribution of the parameters to the physical nature of the formula?

- $\frac{Q}{Q_{hi}}$ This term captures the bed evolution. The discharge is averaged over a period of 50 days, which is the median turnover time for bedforms to adapt to new flow conditions. The added value of the discharge history is clear as it increases the uniformity in the 2D dune statistics – discharge relation. The discharge history term 'explains' the geometry bedforms with respect to the moment of measuring.
- Dune steepness $\frac{H}{L}$. Van Rijn already included this term in his equation for estimating bedform roughness. In addition, this term is already implicit in the equation in the term $h^{-0.3}$. However, since static steepness is assumed here by using the water depth term , a dynamic steepness based on bed measurement has also been added to the formula. The higher this ratio, the more roughness a dune causes. This term seemed important to improve the r^2 of the formula fits.
- The powers of the added terms in the formula have no physical source. They only regulate the contribution of the dimensionless added fractions to avoid too many outliers. The fixed coefficient in the exponent, 6.2, also has no physical explanation as it only affects the shape of the exponential function. This was also the case in the development of the formula by Niesten et al. (2022).The coefficient in front of the equation was allowed to vary randomly. However, it appears that this coefficient follows approximately the same trend as the mean dune height in the three assessed sections, as can be seen in Figure 27. The small step in mean dune height from section 1 to section 2 can also be observed in the coefficient. The

same holds for the transition from section 2 to section 3. This means that a comparable approach can be used to determine this coefficient as in Niesten et al. (2022), where the variable A (see Equation 2) was a scaled version of the dune height.

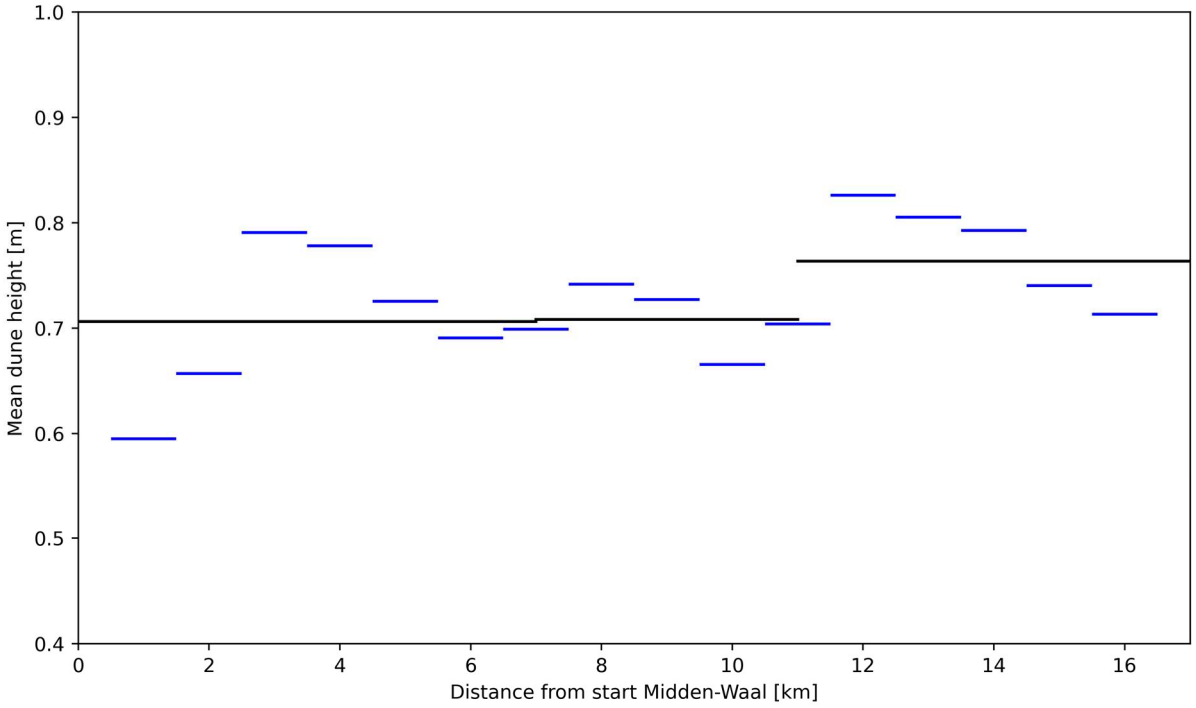

Figure 27 Mean dune height in the Midden-Waal. The sections are based on the spatial characteristics of the background roughness and the roughness multipliers in the standard model. Dune height is averaged over all available data and, unlike earlier in this study, no distinction is made between discharge ranges.

4. Discussion and recommendations

In this chapter the discussion and the recommendations can be found. First, the discussion is done for the used data, the main assumption in this research and the method and results per research question. Than, recommendations will be done for further research.

4.1 Data

The main input for this study was the multibeam bed measurement dataset of the Midden-Waal. As the bed was measured approximately every two weeks, the bed development in between could not be used to take the study of the influence of discharge history to a higher level. And even if we had more data, the relationship between discharge and bed would be disturbed by shipping and dredging activities, which have a local impact on the bed.
In addition, there was not much bed data available for the times of interest, i.e. periods of high discharge and around discharge peaks. Although there would then be uncertainty due to the uncertainty in the floodplain roughness parameterisation, the conclusions could be carefully extrapolated to the extreme reach. Again, more data are needed to draw better and more complete conclusions.

The same applies to the locations where water levels are measured. At the moment we have to estimate the water level between stations using relatively accurate stage relationship curves. If water levels were measured in more places, it would be possible to calibrate smaller roughness sections more accurately.

4.2 Sources of roughness

The main assumption in this research was that the main channel roughness coefficient was entirely caused by bedforms and that all other sources of roughness were already well captured in the model. This assumption allowed us to establish a relationship between the calibrated main channel roughness coefficient and the 2D bedform statistics derived from multibeam measurements. Bedform roughness is thought to be the main source of river roughness (Paarlberg et al., 2010; de Lange et al., 2021). However, the actual contribution of bedforms to the actual roughness is not known (de Lange et al., 2021). It therefore remains uncertain how physically based the new roughness relationships are if only bedforms are considered to be important. The value of this research can therefore only be determined if the discharge dependent contribution of the main channel bed roughness is known, which requires some complicated research.

4.3 RQ 1: 2D dunes vs 3D dunes

This study attempted to create a 3D representation of the river bed. However, this representation did not appear to be usable yet: In the 2D approach, dunes are connected by a trough, a clear point of separation. This was not the case in the 3D approach, where the size was determined by a certain percentile of the bed elevation. Troughs were not defined and therefore a clear separation between two adjacent dunes was difficult to make. In particular, the definition of the dune area appeared to be difficult.
This does not mean that 3D dune statistics are not useful, as a better representation of the bed increases the possibility to better define bedform induced roughness. If dune area, dune volume, dune length and dune width are well defined, better roughness estimates can be made when these

geometry parameters are combined with results from field measurements or high resolution flow simulations around different bedforms.

4.4 RQ 2: Discharge history

In this study, the discharge history was added to the existing main channel roughness formula in Delft3D. This increased the physical nature of the roughness estimate by implicitly including dynamic bedforms. In the ideal case, (small scale) morphological changes are modelled directly in Delft3D instead of implicitly as a function of water depth or discharge. However, this is not yet feasible due to lack of computing power.
An important element in adding the discharge history is the time over which the discharge is averaged. As bed measurements were available for an interval of approximately 14 days, short term bed evolution was not considered in this research. If this had been the case, the discharge history fraction Q/Qhis could have been validated for short-term bed development. This is not possible for the current dataset.
The best fits to the roughness estimates were obtained with a discharge history averaged over 50 days. This could be related to the mean bedform turnover time (Zomer et al., 2021). In this way a general correction is made based on the discharge history, but ultimately the interaction of the bed with the flow cannot be captured in a simple fraction with the averaged discharge over 50 days. A combination of long and short term discharge may be an improvement, but this was beyond the scope of this study.

4.5 RQ 3: New roughness sections

The calibration of the new roughness sections based on the spatial trend of dune height in the Midden-Waal did not lead to improvements in the estimation of main channel roughness. It is not known whether the conversion of the water level time series via the stage relation curves caused some problems or whether there were still some errors in the complicated OpenDA configuration. However, this seems unlikely as the calibration gave satisfactory results, except for the unexplained peak around 1350 m3/s. This peak made it impossible to relate the 2D statistics to the calibration main channel bed roughness.
Peaks in calibrated roughness are common (Domhof et al., 2018). This study concluded that not all peaks can be related to bedform dynamics. River geometry can cause peaks in the discharge-roughness relationship as the discharge enters the floodplain. However, no peaks were observed around 1350 m3/s in Domhof et al. (2018) and no links between geometry, hydraulic radius or flow area could be used to explain this peak.

4.6 Validation and applicability research

The results of this research are at least valid for the Midden-Waal. The results can be generalised to the whole Waal after validation. For this purpose, 2D dune statistics should be derived for the whole Waal and a relation between the free coefficient in the final roughness estimation formula and the dune height should be established. The derived roughness estimation formula can then be used to estimate the main channel bed roughness. Plots and statistics similar to the NRMSE can be used to analyse the performance of the derived formula in this study. If the results are positive, this approach could be applied to other dune dominated riverbeds.

4.7 Recommendations:

Based on the discussion and the context of the research, some recommendations for further research are defined:

1. Improve the parameterisation of the river bed by using 3D bedform parameters. In this study an attempt was made to create a 3D representation of the river bed. However, this

representation did not describe the reality well. However, further research should be carried out to determine whether a 3D parameterisation of the bed is an enrichment of the 2D approach. A clear advantage of the 3D approach is that it does not require unnecessary data processing, as 3D parameters can be extracted more easily than parameters from a 2D river bed parameterisation.

2. Much research has been done on the sources of roughness in rivers. However, it is difficult to generalise the results and apply them in the field. Therefore, knowledge of other sources of roughness should also be improved before the main channel (bed) roughness parameterisation can be improved.
   Research into the contribution of different roughness sources can be carried out using reverse engineering, which makes it easier to distinguish between different contributions to roughness once more data from different roughness sources have been collected. One of the elements that could give us new insights into the relationship between discharge and roughness sources is the calibration procedure:
3. Calibration of the main channel roughness parameter ensures that water levels can be reproduced for the discharge time series for which the calibration is performed. The effect of hysteresis in roughness has not yet been accurately captured (van Leeuwen & Bom, 2019) The relationship between bedforms and calibrated roughness can be improved by calibrating the same discharge levels several times with different time series, which is likely to result in slightly different values for the calibrated roughness, especially if the bedforms are different for the different calibration time series. It is recommended to start by analysing the relationship between bedforms and different discharge time series, as the river bed is the most dynamic factor in the sources of roughness. The next step can be to assess the floodplain roughness using the same methodology.

5. Conclusion

The goal of this study was to answer the following main question:

1. To what extent does the use of 3D bed parameterisation statistics, as opposed to 2D dune statistics, provide additional information that reduces the degree of calibration?
2. To what extent does the inclusion of discharge history in the main channel bed roughness parameterisation reduce the degree of calibration required?
3. To what extent does the use of physically based roughness sections help to reduce the degree of calibration required?
4. To what extent can the combined findings from the previous research questions be used to reduce the degree of calibration required for main channel roughness parameterisation?

"To what extent can the current prediction of water levels in rivers by hydraulic models be improved by using bedforms, smaller roughness section and discharge history to estimate the bed roughness for the river Waal?"

Before this question will be assessed, the 4 sub questions are answered.

1. To what extent does the use of 3D bed parameterisation statistics, as opposed to 2D dune statistics, provide additional information that reduces the degree of calibration?

Parametrising the bed roughness with the 3D parameters derived in this study is somewhat premature as the 3D parameters were obtained with a method which has not the scientific substantiation as the 2D dune parameters have.
Improvements in the derivation of these 3D statistics will increase the physical value of these parameters and may therefore also increase the physical value of bedform induced roughness as more aspects of the flow over and around bedforms can be captured. The use of a 3D approach also facilitates the processing of multibeam measurements into bedform parameters, as no conversion to a data format from which 2D parameters can be extracted is required.

2. To what extent does the inclusion of discharge history in the main channel bed roughness parameterisation reduce the degree of calibration required?

The existing simplified van Rijn formula was extended to include a discharge history dependent term to capture the effects of discharge history on bed development. The inclusion of discharge history improves the physical nature of the formula as bedform dynamics are included better. The extended roughness estimate formula approximates the calibrated roughness in the Midden-Waal much better than the roughness estimate in the default model ('worst' improvement: NRMSE of 0.94 to 0.31)
The best fits were obtained with a discharge history of 50 days, which is the median bedform turnover time. Sensitivity analysis of longer of shorter discharge history periods showed less added value of the discharge history, which means that the length of the discharge history should be chosen wisely.
Analysis of 2D dune statistics showed that the dune steepness H/L might be useable as parameter in the final roughness formula, established in the last research question as it increased nicely with discharge.

3. To what extent does the use of physically based roughness sections help to reduce the degree of calibration required?

New roughness sections were determined based on the spatial trend in dune height in the Midden-Waal. No clear trend was found between the calibrated main channel roughness for the 3 discharge ranges and the dune height in each of these discharge ranges, mainly caused by a peak in the calibrated roughness. This peak could not be explained by using bedform dynamics or river geometry. The new calibrated roughness sections are therefore not (yet) useful for improving the description of the river bed.

4. To what extent can the combined findings from the previous research questions be used to reduce the degree of calibration required for main channel roughness parameterisation?

Discharge history, dune steepness and the roughness section in the default model were used to built a final roughness formula. The combination of discharge history and dune steepness appeared to strengthen each other. The final roughness formula was established for the three roughness sections in the Midden-Waal and resulted in NRMSE values of 0.192, 0.083 and 0.090 respectively. This shows that the default roughness estimate has been improved significantly.
Analysis of the 2D statistics in this final roughness estimate formula showed that the discharge – dune statistics relation was much improved by the presence of the discharge history.

It can be concluded that the estimates of main channel roughness in the Midden-Waal can be improved. By using reverse engineering, discharge history, 2D bedform statistics and calibrated roughness were used to establish a new roughness formulation which performs reasonably accurate between 600 m^3/s and 1900 m^3/s. The degree of required calibration was significantly decreased with respect to the default roughness estimate.

Bibliography

Bartholdy, J., Flemming, B. W., Ernstsen, V. B., Winter, C., & Bartholom ä, A. (2010). Hydraulic roughness over simple subaqueous dunes. *Geo-Marine Letters*, *30*(1), 63–76. https://doi.org/10.1007/s00367-009-0153-7

Berends, K. D., Warmink, J. J., & Hulscher, S. J. M. H. (2018). Efficient uncertainty quantification for impact analysis of human interventions in rivers. *Environmental Modelling and Software*, *107*, 50–58. https://doi.org/10.1016/j.envsoft.2018.05.021

Bomers, A., Schielen, R. M. J., & Hulscher, S. J. M. H. (2019). The influence of grid shape and grid size on hydraulic river modelling performance. *Environmental Fluid Mechanics*, *19*(5), 1273–1294. https://doi.org/10.1007/s10652-019-09670-4

Bradley, R. W., & Venditti, J. G. (2017). Reevaluating dune scaling relations. In *Earth-Science Reviews* (Vol. 165, pp. 356–376). Elsevier B.V. https://doi.org/10.1016/j.earscirev.2016.11.004

Bridge, J. (2003). Rivers and Floodplains: Forms, Processes and Sedimentary Record, Malden. *SERBIULA (Sistema Librum 2.0)*.

de Lange, S. I., Naqshband, S., & Hoitink, A. J. F. (2021). Quantifying Hydraulic Roughness From Field Data: Can Dune Morphology Tell the Whole Story? *Water Resources Research*, *57*(12). https://doi.org/10.1029/2021WR030329

Domhof, B., Berends, K. D., Spruyt, A., Warmink, J. J., & Hulscher, S. J. M. H. (2018). Discharge and location dependency of calibrated main channel roughness: Case study on the River Waal. *E3S Web of Conferences*, *40*. https://doi.org/10.1051/e3sconf/20184006038

Engelund, F. (1977). *Hydraulic resistance for flow over dunes. Progress report 44, Institute for Hydrodynamic and Hydraulic Engineering, Technical University of Denmark*.

Haase, J. R., Lokin, L. R., Warmink, J. J., & Daggenvoorde, R. (2023). Analysing the spatio-temporal variability of river dune induced roughness for the Midden-Waal. In W. C. F. Verberk & G. Geerling (Eds.), *Towards 2048: the next 25 years of river studies* (pp. 48–49). Radboud University.

Hardy, R. J., Bates, P. D., & Anderson, M. G. (1999). The importance of spatial resolution in hydraulic models for floodplain environments. *Journal of Hydrology* , *216*, 124–136.

Horritt, M. S., & Bates, P. D. (2002). Evaluation of 1D and 2D Numerical Models for Predicting River Flood Inundation. *Journal of Hydrology*, *268*, 87–99. https://doi.org/10.1016/S0022-1694(02)00121-X

Huang, S., Krysanova, V., & Hattermann, F. (2015). Projections of climate change impacts on floods and droughts in Germany using an ensemble of climate change scenarios. *Regional Environmental Change*, *15*(3), 461–473. https://doi.org/10.1007/s10113-014-0606-z

Lefebvre, A., & Winter, C. (2016). Predicting bed form roughness: the influence of lee side angle. *Geo-Marine Letters*, *36*(2), 121–133. https://doi.org/10.1007/s00367-016-0436-8

Lokin, L. R., Warmink, J. J., Bomers, A., & Hulscher, S. J. M. H. (2022). River Dune Dynamics During Low Flows. *Geophysical Research Letters*, *49*(8). https://doi.org/10.1029/2021GL097127

McElroy, B., & Mohrig, D. (2009). Nature of deformation of sandy bed forms. *Journal of Geophysical Research: Solid Earth*, *114*(3). https://doi.org/10.1029/2008JF001220

Naqshband, S., Hoitink, A. J. F., McElroy, B., Hurther, D., & Hulscher, S. J. M. H. (2017). A Sharp View on River Dune Transition to Upper Stage Plane Bed. *Geophysical Research Letters*, *44*(22), 11,437-11,444. https://doi.org/10.1002/2017GL075906

Neal, J., Schumann, G., & Bates, P. (2012). A subgrid channel model for simulating river hydraulics and floodplain inundation over large and data sparse areas. *Water Resources Research*, *48*(11). https://doi.org/10.1029/2012WR012514

Niesten, I., Spruyt, A., & Kosters, A. (2022). *Ontwikkeling zesde-generatie Rijntakken model Modelbouw, kalibratie en validatie - Deltares*.

Paarlberg, A. J., Dohmen-Janssen, C. M., Hulscher, S. J. M. H., Termes, P., & Schielen, R. (2010). Modelling the effect of time-dependent river dune evolution on bed roughness and stage. *Earth Surface Processes and Landforms*, *35*(15), 1854–1866. https://doi.org/10.1002/esp.2074

Parmet, B., Kwadijk, J., & Raak, M. (1995). Impact of climate change on the discharge of the river rhine. *Studies in Environmental Science*, 911–918.

Reesink, A. J. H., Parsons, D. R., Ashworth, P. J., Best, J. L., Hardy, R. J., Murphy, B. J., McLelland, S. J., & Unsworth, C. (2018). The adaptation of dunes to changes in river flow. In *Earth-Science Reviews* (Vol. 185, pp. 1065–1087). Elsevier B.V. https://doi.org/10.1016/j.earscirev.2018.09.002

Rijkwaterstaat. (2023, July 7). *Betrekkingslijnen Rijn*. https://www.helpdeskwater.nl/@245949/betrekkingslijnen-rijn/

Soulsby, R. (1997). *Dynamics of marine sands. A manual for practical applications* (Vol. 9).

van Leeuwen, B., & Bom, S. (2019). *Opstellen Qf relaties 2018 Data-analyse en modelstudie*. www.svasek.com

Van Rijn, L. C. (1984). Sediment transport, Part III: Bed forms and alluvial roughness. *Journal of Hydraulic Engineering*, *110*(10), 1431–1456. https://doi.org/https://doi.org/10.1061/(asce)0733-9429(1984)110:12(1733)

Vanoni, V. A., & Hwang, L. S. (1967). BED FORMS AND FRICTION IN STREAMS. *Journal of Hydraulic Engineering*.

Warmink, J. (2011). *Unraveling uncertainties : the effect of hydraulic roughness on design water levels in river models*. s.n.]. https://doi.org/10.3990/1.9789036532273

Warmink, J. (2014). Dune dynamics and roughness under gradually varying flood waves,. *Copernicus Publications*. https://doi.org/https://doi.org/10.5194/adgeo-39-115-2014

Warmink, J., Booij, M. J., Van der Klis, H., & Hulscher, S. J. M. H. (2013). Quantification of uncertainty in design water levels due to uncertain bed form roughness in the Dutch river Waal. *Hydrological Processes*, *27*(11), 1646–1663. https://doi.org/10.1002/hyp.9319

Zomer, J. Y., Naqshband, S., Vermeulen, B., & Hoitink, A. J. F. (2021). Rapidly Migrating Secondary Bedforms Can Persist on the Lee of Slowly Migrating Primary River Dunes. *Journal of Geophysical Research: Earth Surface*, *126*(3). https://doi.org/10.1029/2020JF005918

Appendix A: Calibration

```
<?xml version="1.0" encoding="UTF-8"?>
<DudConfig  xmlns="http://www.openda.org" xmlns:xsi="http://www.w3.org/2001/XMLSchema-instance"
xsi:schemaLocation="http://www.openda.org http://schemas.openda.org/algorithm/dudConfig.xsd">
    <costFunction weakParameterConstraint="true" class="org.openda.algorithms.SimulationKwadraticCostFunction" stdRemoval="true" /><!-
    <outerLoop maxIterations="10" absTolerance="0.001" relTolerance="0.001" relToleranceLinearCost="0.0001" />
    <lineSearch maxIterations="5" maxRelStepSize="10.0" >
        <backTracking shorteningFactor="0.5" startIterationNegativeLook="3" />
    </lineSearch>
    <stopCriteria>
        <stopCriterion class="org.openda.algorithms.AbsoluteAveragePerLocationStopCriterion" threshold="0.02" />    <!-- drempel -->
    </stopCriteria>
    -->
    <observationFilters>
    <observationFilter class="org.openda.algorithms.DischargeDependentFilter">
        <workingDirectory>.</workingDirectory>
        <configFile>dischargeDependentObservationFilter_H1.xml</configFile>
    </observationFilter>

    <observationFilter class="org.openda.algorithms.AssimilationObservationFilter" />
</observationFilters>
</DudConfig>
```

Figure 28 Calibration setttings

```
#-------------------------------------------------------------------------------
2003 DISCHARGE WL_876.6_QR_Pannkop-Nijmegen # Pannkop-Nijmegen
2003 0800 0.948
2003 1580 0.942
2003 2070 0.969
2003 2700 0.969
2003 5350 0.998
2003 7200 0.943
#-------------------------------------------------------------------------------
2004 DISCHARGE WL_894.8_QR_Nijmegen-Dodewaard # Nijmegen-Dodewaard
2004 0800 0.854
2004 1580 0.907
2004 2700 0.94
2004 5350 0.942
2004 7200 0.897
#-------------------------------------------------------------------------------
2005 DISCHARGE WL_910.4_QR_Dodewaard-Tielwaal # Dodewaard-Tielwaalkm911
2005 0800 0.848
2005 1580 0.936
2005 2700 1.001
2005 5350 1.03
2005 7200 0.981
#-------------------------------------------------------------------------------
2006 DISCHARGE WL_924.3_QR_Tielwaal-Zaltbommel # Tielwaalkm911-Varik
2006 0900 0.883
2006 1580 0.982
2006 2700 1.076
2006 5350 1.033
2006 7200 0.892
#-------------------------------------------------------------------------------
```

Figure 29 Spatially varying calibration factors (Cfac) for 6 discharge levels in the Midden-Waal.

Appendix B: Discharge coefficients

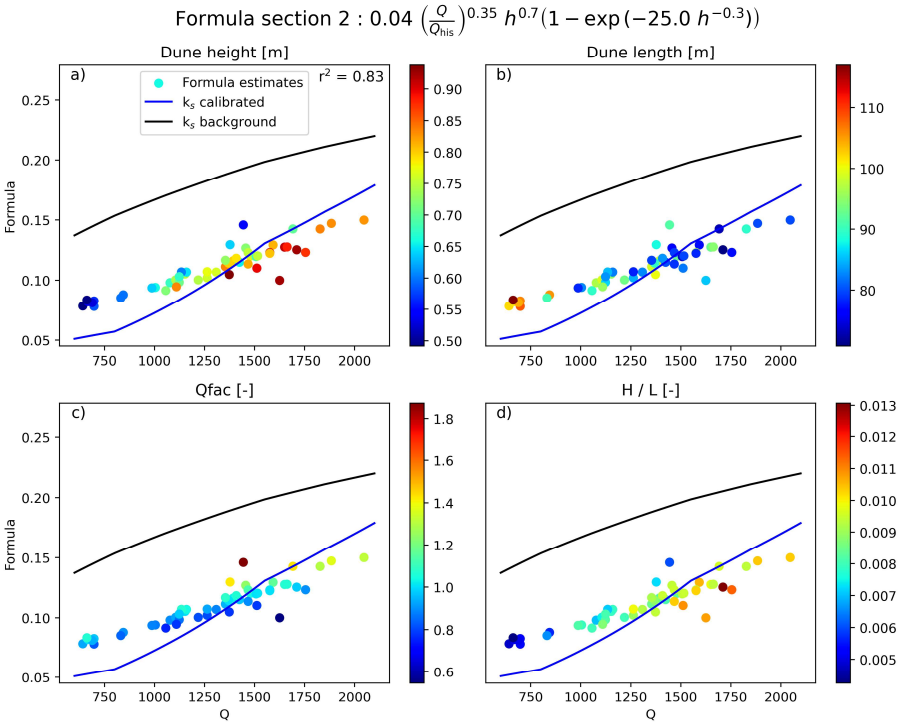

Figure 30 New roughness formula section 2

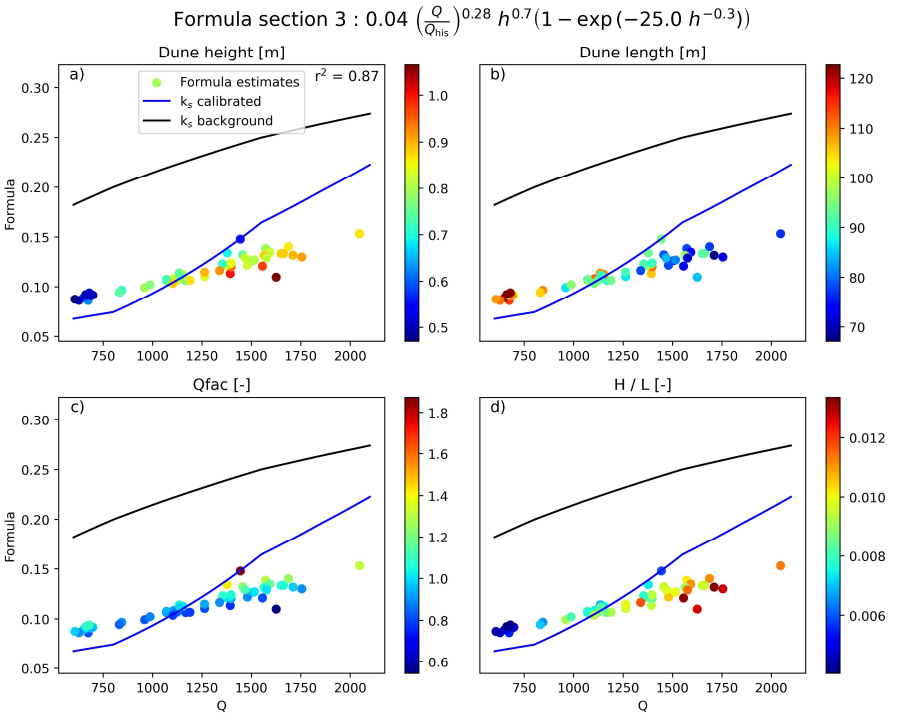

Figure 31 New roughness formula section 3

Appendix C: Reverse engineering

A recurring element in this research was the reverse engineering approach. Due to the assumption that all the main channel roughness in the Midden-Waal can be attributed to bed forms, the calibrated roughness in the model provided by Deltares (this will be called the '**default model'** from now) could be used as a target to establish a new roughness parametrization. Figure 32 shows schematically how this was applied. The goal of this research was to improve the roughness estimate in D-HYDRO by a new parametrization which was closer to calibrated roughness in the default model (EQ. 1).

The three boxes on the top row correspond with the 3 research questions. In each of these questions, the required degree of calibration was tried to be reduced by trying to find relations between the subject in question and the calibration roughness as target. The formula building that was done in RQ 2 and 4 was limited to the fixed set of optional roughness formulas in D-HYDRO (Niesten et al., 2022). Adding new formulas is not possible.

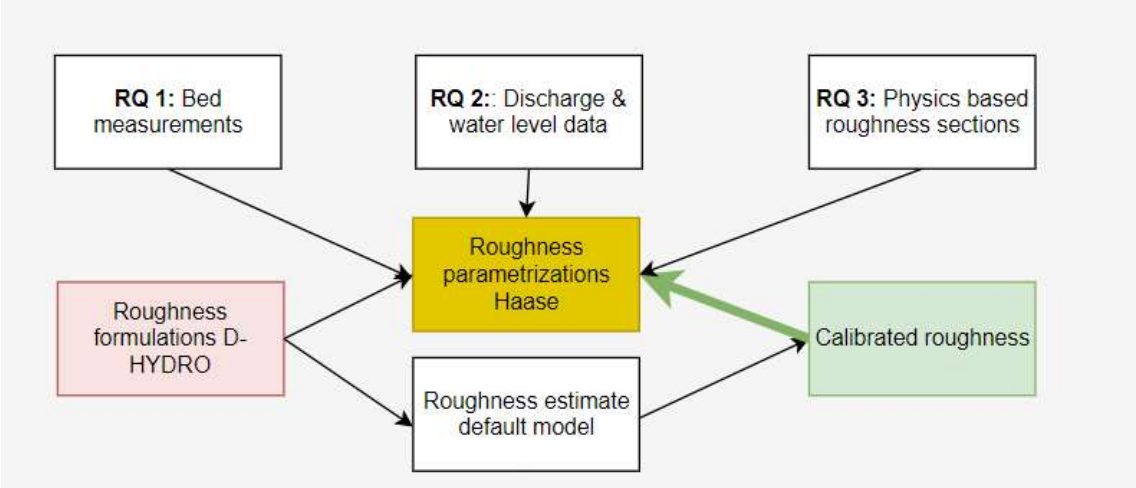

Figure 32 Reverse engineering